

~~The Modeling the~~ spatially distributed nature of subglacial sediment dynamics: using a numerical model to quantify sediment transport and bedrock erosion across a glacier bed in response to glacier behavior and hydrology

Ian Delaney¹, Leif S. Anderson^{1,2}, and Frédéric Herman¹

¹Institut des dynamiques de la surface terrestre (IDYST), Université de Lausanne, Bâtiment Géopolis, CH-1015 Lausanne

²Department of Geology and Geophysics, University of Utah, Frederick Albert Sutton Building, 115 S 1460 E, Salt Lake City, UT 84112-0102, USA

Correspondence: Ian Delaney (IanArburua.Delaney@unil.ch)

Abstract. In addition to ice and water, glaciers expel sediment. As a result, changing glacier dynamics and melt will result in changes to glacier erosion and sediment discharge, which can impact the landscape surrounding retreating glaciers, as well as communities and ecosystems downstream. To date, the available models of subglacial sediment transport on the sub-hourly to ~~decadal-scale exist~~ decadal scale transport sediment in one dimension, usually along a glacier's flow line. Such models have proven useful in describing the formation of landforms, the impact of sediment transport on glacier dynamics, the interactions between climate, glacier dynamics, and erosion. However, ~~because of the large role of sediment connectivity in determining sediment discharge~~ in one dimension, these models omit the two-dimensional spatial distribution of sediment and its impact on sediment connectivity, the movement of sediment between its detachment in source areas and its deposition in sinks. In turn, the geoscience community needs modeling frameworks that describe subglacial sediment discharge in two spatial dimensions (x and y) over time. Here, we present SUGSET_2D, a numerical model that evolves a two-dimensional subglacial till layer in response to the erosion of bedrock and changing sediment transport conditions below ~~the glacier. Experiments employed on test cases of synthetic ice sheets and alpine glaciers~~ glaciers. Experiments performed using an idealized alpine glacier demonstrate the heterogeneity in sediment transport across a glacier's bed. Furthermore, the experiments show the and bedrock erosion below glaciers. The experiments show a non-linear increase in sediment discharge following increased glacier melt. ~~Lastly, we~~ We also apply the model to ~~Griesgletscher in the Swiss Alps where we use a parameter search to test model outputs against a real alpine glacier. We compare simulations with~~ annual observations of sediment discharge measured from ~~the glacier. The model captures the glacier's inter-annual variability and quantities of sediment discharge . Furthermore, the Griesgletscher in the Swiss Alps. SUGSET_2D reproduces the year-to-year sediment discharge pattern measured at the glacier terminus. The model's~~ capacity to represent ability to match the data depends greatly on the sediment grain size parameter, which controls subglacial sediment transport capacity. Smaller grain ~~size of sediment . Smaller sediment~~ sizes allow sediment transport to occur in regions of the bed with reduced water flow and channel size, effectively ~~increases~~ increasing sediment connectivity into the main channels. Model outputs from ~~the three test cases together~~ both cases show the importance of

considering heterogeneities in water discharge and sediment ~~availability in two dimensions~~transport in both the x - and y -dimensions.

25 1 Introduction

Increasing glacier ablation ~~will change~~perturbs the ways that glaciers erode bedrock and supply sediment ~~to downstream sources (e.g. Church and Ryder, 1972; Lane et al., 2017; Milner et al., 2017). In the Alps already, increased fluxes of sediment in the Rhône Valley have been identified at the basin scale in response to increased glacier melt (Costa et al., 2018; Lane et al., 2019).~~
30 ~~Changes to sediment discharge have also been identified in the Arctic, where large proglacial deltas have grown off the coast of Greenland in recent decades (Bendixen et al., 2017).~~

~~The impact of changes to sediment discharge from glaciers on mountains or high-latitude landscapes, as well as~~downstream (e.g. Church and Ryder, 1972; Lane et al., 2017; Delaney and Adhikari, 2020). Changing sediment discharge from glaciers in alpine and polar landscapes impacts many downstream social and earth systems ~~implies a need for predictive models (Milner et al., 2017; Li~~
~~. In turn, predictive models are needed~~ to understand the response of these systems to glacier retreat. In alpine ~~environments~~environment,
35 increased sediment discharge ~~results in the in-fill of proglacial hydropower~~leads to the more rapid filling of proglacial reservoirs (Thapa et al., 2005) and ~~abrasion~~the abraiding of hydropower infrastructure (e.g. Felix et al., 2016). ~~Additionally, the~~The flux of sediment from glaciers also dramatically alters alpine ecosystems (Milner et al., 2017). In the Arctic, increased sediment discharge can affect biogeochemical cycles given that sediments may carry phosphorus and iron (Bhatia et al., 2013; Hawkings et al., 2014). These elements ~~limit bio-availability in the Arctic~~are limiting nutrients in the oceanic ecosystem, so any change to
40 sediment discharge from the ice sheet ~~may substantially~~can alter Arctic ecosystems (Wadham et al., 2019). Modeling studies and observations suggest that increases in sediment output from alpine glaciers could occur when high melt extends up-glacier ~~allowing sediment transport where no sediment could be transported before (Lane et al., 2017; Delaney and Adhikari, 2020)~~
~~mobilizing sediment in new areas (Lane et al., 2017; Delaney and Adhikari, 2020; Li et al., 2021).~~

Generally, two processes determine the sediment discharge below ~~a glacier by adding or removing sediment from a subglacial~~
45 ~~till layer~~glaciers: one process adds sediment, the other removes sediment from subglacial till layers (Figure 1; Brinkerhoff et al., 2017; Delaney et al., 2019). Bedrock erosion adds material to the subglacial till layer. Bedrock erosion ~~occurs~~is accomplished by quarrying, when pressure differentials on opposing sides of obstacles cause fractures to expand and rock to detach (Iverson, 1990; Alley et al., 1997; Hallet et al., 1996; Iverson, 2012), and abrasion, when debris embedded in the ice grinds bedrock as the glacier slides above (Hallet, 1979; Alley et al., 1997). ~~Physically describing these processes requires evaluating~~
50 ~~Representing these physical processes in models requires independent knowledge of~~ a large number of parameters (c.f. Ugelvig et al., 2018), so many researchers use empirical relationships that relate glacier sliding to glacier erosion ~~. In doing so they represent processes such as abrasion and quarrying in their models (Humphrey and Raymond, 1994; Koppes et al., 2015; Herman et al., 2015).~~
~~This sliding relationship (Humphrey and Raymond, 1994; Koppes et al., 2015; Herman et al., 2015; Cook et al., 2020). The sliding relationship with glacier erosion~~ proves especially useful ~~in applications when applied~~ over large temporal and spa-
55 tial scales, ~~such as evaluating the interaction to~~ for example, explore the coupling between glacier erosion and ~~tectonics~~

(e.g. Egholm et al., 2009; Prasicek et al., 2018; Herman et al., 2018; Prasicek et al., 2020) tectonic uplift (e.g. Egholm et al., 2009; Prasicek et al., 2020)

Conversely, fluvial mobilization can remove sediment from the till layer below the glacier (e.g. Walder and Fowler, 1994; Ng, 2000; Creyts et al., 2013). When pressurized subglacial water sediment transport removes material from subglacial till layers (e.g. Walder and Fowler, 1994; Ng, 2000) or may deposit it there (e.g. Beaud et al., 2018b). When subglacial water velocity increases above a critical velocity, then substantial amounts of sediment of a given grain size begin to be transported (Shields, 1936). However, the amount of sediment that may be mobilized given sediment transport conditions depends on the presence of sediment (e.g. Mao et al., 2014). In this way, sediment is transported downvalley, and if the water velocity slows below the threshold sediment may be deposited (Shields, 1936). The sediment mobilization ceases when no sediment is present, and the system is supply-limited (e.g. Mao et al., 2014). It follows that fluvial sediment transport depends both on the subglacial hydraulic characteristics (e.g. Walder and Fowler, 1994), as well as the availability of sediment at the glacier bed (e.g. Willis et al., 1996; Swift et al., 2005).

Bedrock erosion and fluvial sediment transport vary depending on the timescales and characteristics of individual glaciers. For instance, erosive processes likely dominate over sediment transport processes on characteristics of each glacier. Bedrock erosion tends to dominate sediment transport below glaciers with minimal sediment storage, large concentrations of subglacial debris entrained at the glacier sole and steep gradients (Humphrey and Raymond, 1994; Herman et al., 2015, 2021). Furthermore, landscape evolution models that use empirical relationships to quantify erosion with respect to sliding speed, (Hallet, 1979; Humphrey and Hallet, 2002). Landscape evolution models that represent glacier landscapes demonstrate the dominant role of erosional processes, as opposed to sediment transport processes, over geologic timescales (Harbor et al., 1988; Herman et al., 2011; Egholm et al., 2012). Conversely, over shorter timescales of months to decades, and on shallower glaciers, fluvial sediment transport is a key driver often drives sediment discharge from glaciers (e.g. Delaney et al., 2018b; Perolo et al., 2018; Delaney et al., 2019).

Numerical implementation of The development of numerical models of subglacial sediment transport thus far has focused on one-dimensional models (e.g. Creyts et al., 2013; Beaud et al., 2018a; Hewitt and Creyts, 2019; Delaney et al., 2019). These frameworks have yielded foundational insights into the creation of eskers (Beaud et al., 2018a; Hewitt and Creyts, 2019), the formation of subglacial canals through which water flows (Walder and Fowler, 1994; Ng, 2000; Kasmalkar et al., 2019) and the behavior of tidewater glaciers (Brinkerhoff et al., 2017). Additionally, a subglacial sediment transport model demonstrates processes by which an over-deepened glacier bed causes sediment to be deposited on its adverse slope (Creyts et al., 2013). It is also been possible to reproduce measurements of sediment discharge using a subglacial sediment transport model (Delaney et al., 2019).

At the same time, sediment connectivity, the transfer of sediment from source to sink, plays a fundamental role in sediment discharge (Figure 1; e.g. Braeken et al., 2015; Micheletti and Lane, 2016; Wohl et al., 2019; Mancini and Lane, 2020). Here, the have thus far focused on processes acting a single downglacier (x -) dimension. Yet, the spatial heterogeneities in the distribution of sediment and sediment transport capacity (largely controlled by water velocity) often result in less sediment being carried by the water than could be theoretically transported (e.g. Lane et al., 2017; Delaney et al., 2018b). As a result, reducing the problem to one dimension omits key processes that control sediment dynamics because subglacial water flows through spatially distributed networks of cavities and channels across the glacier bed (e.g. Werder et al., 2013). Therefore, The

one-dimensional models to date models have yielded insights into the creation of eskers (Beaud et al., 2018a; Hewitt and Creyts, 2019), the formation of subglacial canals through which water flows (Walder and Fowler, 1994; Ng, 2000; Kasmalkar et al., 2019), subglacial processes in overdeepenings (Creyts et al., 2013) and the behavior of tidewater glaciers (Brinkerhoff et al., 2017). Yet, describing subglacial sediment transport inherently lends itself to a discretization of bedrock erosion, sediment transport, water flow, and sediment availability in ~~two spatial dimensions~~ the downstream and transverse dimensions (x and y).

In this manuscript, we present SUGSET_2D, a new two-dimensional subglacial sediment transport model. The model implements subglacial the sediment transport and bedrock ~~erosional processes presented in Delaney et al. (SUGSET; 2019). We apply erosion processes. We implement~~ a routing scheme ~~to the model~~ that transports sediment ~~down-glacier based upon the~~ in x and y based on the local hydraulic potential ~~cases show cases demonstrate~~ the model's ability to reproduce known processes and ~~yields yield~~ ins ~~cc and~~ ~~tributed~~ spatially-distributed processes responsible for subglacial sediment dynamics. ~~Implementation of sediment discharge datasets from the Griesgletscher site that could be generalizable to other situations~~ ~~odel to existing glacier hydrology, topography, and me subglacial sediment transport processes at this gletscher in Switzerland. The model was run with~~ hydrology and topography data from the glacier and ~~charge data are used to validate the model.~~ Through these experiments, we ~~discuss the impact of two dimensional sediment connectivity on subglacial sediment transport~~ explore the importance of two-dimensional sediment connectivity in the subglacial environment.

2 Model Description

The model presented here implements a hydraulic model and sediment routing scheme that translates the one-dimensional subglacial sediment transport model presented in Delaney et al. (2019) to two dimensions. In this section, we review the underpinnings of the model presented in Delaney et al. (2019), describe the routing scheme, and outline its numerical implementation in ~~two-dimension~~ two dimensions.

2.1 Hydraulic Model

SUGSET_2D requires a hydraulics model as a means to route sediment and water through the subglacial environment ~~and~~. The hydraulics model is also needed to evaluate the sediment transport capacity of this water, based upon the hydraulic gradient, channel size and water flux (~~Section 2.2; e.g. Walder and Fowler, 1994; Alley et al., 1997~~) (Table 1, Section 2.2; e.g. Walder and Fowler, 1994). The hydraulic model ~~here~~ is based on the premise that subglacial water flows along the hydraulic potential gradient and ~~glacier~~ that the weight of ice pressurizes water at the ~~glacier~~ bed (Shreve, 1972). We simulate characteristics of an R othlisberger-channel without explicitly describing properties such as creep closure and pressure melt of channel walls.

The hydraulic gradient of a subglacial channel Ψ (at a certain location and time) can be determined with a known hydraulic ~~radius diameter~~ D_h and water discharge Q_w , ~~given~~. The hydraulic gradient can then be determined using the Darcy-Weissbach

equation for fluid flow through a pipe

$$\Psi = s f_r \rho_w \frac{Q_w^2}{D_h^5}. \quad (1)$$

where, s is a factor accounting for channel geometry (Hooke et al., 1990), f_r the density of water is ρ_w , the Darcy-Weisbach friction factor is f_r , and the channel geometry is accounted for by s (Hooke et al., 1990) s can be represented as

$$s = \frac{2(\beta - \sin \beta)^2}{\left(\frac{\beta}{2} + \sin \frac{\beta}{2}\right)^4}, \quad (2)$$

125 where β is the central angle of the circular segment representing the channel edge. Smaller values of β result in broad channels and $\beta = \pi$ results in a semicircular channel. The channel width w_c is given by

$$w_c = 2 \sin \frac{\beta}{2} \sqrt{\frac{2S}{\beta - \sin \beta}}, \quad (3)$$

where S is the Darcy-Weisbach friction factor, ρ_w represents the density of water. Evaluating Ψ in Equation 1 requires prescribing Q_w and D_h . cross-sectional area of the channel given by

$$130 \quad S = \frac{D_h^2}{2} \frac{\left(\frac{\beta}{2} + \sin \frac{\beta}{2}\right)^2}{\beta - \sin \beta}. \quad (4)$$

To approximate the hydraulic diameter D_h , we assign a representative water discharge Q_w^* to Q_w , by taking a quantile of characteristic water discharge over a certain time (e.f. Delaney et al., 2019). This time represents the time period, assumed to be days, over which hydraulic radius D_h evolves in response to period prior (hours to days). We assume that the hydraulic diameter of the channel results from this characteristic water discharge we call the source percentile (c.f. de Fleurian et al., 2018; Delaney et al., 2019).
135 The response time and source percentile remain poorly constrained, yet their impact can be intuited. For instance, short-lived increases in water discharge due to an hour of precipitation will not greatly impact the hydraulic diameter of the subglacial channel, where as prolonged melt would increase the hydraulic diameter.

Water storage is not allowed, such that Q_w^* and Q_w (e.g. Nanni et al., 2020) comprise the total amount of melt water produced upglacier.

140 We then evaluate D_h , the hydraulic radius diameter given

$$D_h = \left(s f_r \rho_w \frac{Q_w^{*2}}{\Psi^*}\right)^{\frac{1}{5}}. \quad (5)$$

Ψ^* is a representative hydraulic gradient at overburden pressure, evaluated using the Shreve potential gradient

$$\Psi^* = \nabla(\rho_i g(z_s - z_b) + \rho_w g z_b), \quad (6)$$

where z_s and z_b are surface and bed elevations, respectively, ρ_i is the density of ice and g is the gravitational acceleration constant.

Now equipped with knowledge of D_h , we insert the instantaneous value of Q_w into Equation 1 to evaluate the instantaneous hydraulic gradient Ψ . In this formulation, we assume that the timescales over which the channel size responds (days) are different than those of instantaneous water discharge (minutes or hours). In this manner, we simulate key characteristics of an R-channel without explicitly describing properties such as creep closure and pressure melt of channel walls.

We note that to prevent unreasonable water pressures when Q_w^* rapidly increases and D_h is small, the model limits the minimal cross-sectional area of D_h to $0.3S$ to 0.5 m^2 .

2.2 Till-layer model: bedrock-bedrock erosion and sediment transport

The model simulates the evolution of a subglacial till layer, which we define as transportable sediment below the glacier due to glacier erosion and fluvial sediment transport. Erosive processes such as abrasion and quarrying add material to the layer. Conversely, fluvial sediment transport mobilizes and deposits sediment, adding or removing material from the till layer (Brinkerhoff et al., 2017; Delaney et al., 2019). To quantify erosive processes such as abrasion and quarrying add material to the layer. To represent these processes, we implement the Exner Equation (Exner, 1920a,b; Paola and Voller, 2005) (Figure 2; Exner, 1920a,b; Paola and Voller, 2005), a mass conservation relationship, to solve for the till layer height given the erosive and fluvial conditions.

$$\underbrace{\frac{\partial H}{\partial t}}_{\text{till evolution}} = \underbrace{\text{bedrock erosion}}_{\text{bedrock erosion}} - \underbrace{\nabla \cdot Q_s}_{\text{sediment transport}} \pm \underbrace{\dot{m}_t}_{\text{bedrock erosion}} \quad (7)$$

H is till thickness and t is time (Table 1). The first term captures bedrock erosion processes, where \dot{m}_t is a bedrock erosion rate. The remaining terms on the right side of the equation represent fluvial sediment transport processes, where Q_s represents sediment transport. $\nabla \cdot Q_s$ represents sediment mobilization in either supply- and/or transport- limited regimes. l is a characteristic length-scale for sediment mobilization, over which sediment mobilization adjusts to sediment transport conditions. The second term captures bedrock erosion processes, where \dot{m}_t is a bedrock erosion rate.

Sediment discharge is calculated. Divergence of the sediment flux is calculated by approximating $\nabla \cdot Q_s$ with $\frac{\nabla \cdot \widetilde{Q}_s}{w}$ and using the mobilization equation from Delaney et al. (2019). scheme from Delaney et al. (2019)

$$\frac{\nabla \cdot \widetilde{Q}_s}{w} = \begin{cases} \frac{Q_{sc} - Q_s}{l} & \text{if } \frac{Q_{sc} - Q_s}{l} \leq \dot{m}_t \text{ and } \frac{Q_{sc} - Q_s}{l} < \dot{m}_t w \\ 0 & \text{if } H = H_{lim} \text{ \& } \frac{Q_{sc} - Q_s}{l} \leq 0 \\ \frac{Q_{sc} - Q_s}{l} \sigma(H) + \dot{m}_t w (1 - \sigma(H)) & \text{otherwise} \end{cases} \quad (8a)$$

$$\text{if } H = H_{lim} \text{ \& } \frac{Q_{sc} - Q_s}{l} \leq 0 \quad (8b)$$

$$\text{otherwise} \quad (8c)$$

w is the width of a patch of glacier bed, perpendicular to the direction of water flow. Q_{sc} is sediment transport capacity, or the amount of sediment that could be transported given hydraulic conditions. l is a characteristic length-scale for sediment mobilization, over which sediment mobilization adjusts to sediment transport conditions. σ is a sigmoidal function

of H

$$\sigma(H) = \left(1 + \exp\left(\frac{2 - \Delta\sigma H}{5}\right) \right)^{-1}, \quad (9)$$

that enables smooth transition over the range: $H = 2\Delta\sigma^{-1} \pm \Delta\sigma^{-1}$ in Equation 8c. $\Delta\sigma$ is a value below which σ substantially deviates from 1, and reduces sediment mobilization.

170 Condition 8a represents the case where bedrock erosion exceeds sediment mobilization, thus sediment transport exists in a transport -limited regime. ~~In Condition 8b , impedes sediment transport impedes mobilization or deposition, transporting sediment~~ to the next cell when a till thickness is equal to H_{lim} , the value of which is chosen to be on the order of maximal change in till height over the model run (~ 10 cm). This term prevents unbounded sediment accumulation ~~in over-deepenings where excessive deposition can occur (Alley et al., 2003). Mechanisms to capture processes occurring in over-deepenings are not included in the model,~~ as the model does not include physical processes to limit sediment deposition, such as reduced channel size in response to infill of sediment (Perolo et al., 2018). Condition 8c allows sediment mobilization to ~~occur over a smoothly transition~~ between transport- and supply-limited regimes. ~~In this case, when H is small, sediment mobilization is limited to the,~~ limiting sediment mobilization to sediment production term \dot{m}_t (see below), when H is small.

We calculate sediment transport capacity Q_{sc} using the total sediment transport relationship by Engelund and Hansen (1967),
180

$$Q_{sc} = \frac{0.4}{f_r} \frac{1}{D_{m50} \left(\frac{\rho_s}{\rho_w} - 1\right)^2 g^2} \frac{1}{D_m \left(\frac{\rho_s}{\rho_w} - 1\right)^2 g^2} \left(\frac{\tau}{\rho_w}\right)^{\frac{5}{2}} w_c, \quad (10)$$

where ρ_s (ρ_w) is the bulk density of the sediment (water), ~~D_{m50}~~ D_m is the mean sediment ~~grain-size,~~ w_c ~~denotes width of the channel floor that integrates the sediment transport rate across the width of the channel (c.f. Delaney et al., 2019)~~ grain size and τ represents the shear stress between the water and the channel bed. We determine the shear stress through the Darcy-Weisbach
185 formulation:

$$\tau = \frac{1}{8} f_r \rho_w v^2, \quad (11)$$

where $v = \frac{Q_w}{S}$ is the water velocity and S is evaluated in Equation 1. ~~We note that because Engelund and Hansen (1967)'s formulation relies on shear stress, other~~ Other sediment transport relationships using shear stress could be exchanged by the model operator (e.g. Meyer-Peter and Müller, 1948). We chose Engelund and Hansen (1967)'s formulation due to the
190 representation of both suspended and bedload transport. ~~Furthermore, the continuous nature of the relationship improves the model stability.~~

Source term \dot{m}_t is described as,

$$\dot{m}_t = \dot{e} \left(1 - \frac{H}{H_{max}} \right), \quad (12)$$

where H_{max} is a till height beyond which no further erosion, \dot{e} may occur.

We chose to use an empirical relationship with sliding velocity u_b to describe bedrock erosion,

$$\dot{e} = k_g u_b^{l_{er}}, \quad (13)$$

195 k_g is an erodability constant and l_{er} is an exponent, which varies from between 0.66 and 3 (Herman et al., 2021). u_b is assumed to be a given fraction f_{sl} of the ice deformation velocity (e.g. Weertman, 1957), and is calculated via the shallow ice approximation (Hutter, 1983): relates to basal shear stress (τ_b ; Weertman, 1957) given the following relationship

$$u_{bb} = \frac{f_{sl} \frac{2A}{n+1} (\rho_i g \sin \alpha)^n (z_s - z B \tau_b)^{n+1} \cdot m}{}, \quad (14)$$

Here, n is the exponent in Glen's, A is the ice flow rate factor, B is a constant and we assume the exponent m is equal to 1. We assume that τ_b is equal to driving stress (Cuffey and Paterson, 2010)

$$\tau_b = \rho_i g h (\sin \alpha), \quad (15)$$

200 where ρ_i is the density of ice, h is the glacier thickness and α is the surface slope of the glacier.

Note that because \dot{m}_t is a source term, alternative parameterizations of erosion or basal sliding can easily be exchanged, as we do in some cases below.

2.3 Spatial and temporal discretization, and parameters

Here, we describe the numerical implementation of the equations presented above, and in particular the routing scheme that
205 enables a two-dimensional two-dimensional representation of subglacial fluvial and till dynamics.

2.3.1 Routing algorithm and Numerical implementation and parameters

Sediment and water are routed down the hydraulic gradient using a multi-cell routing scheme (Quinn et al., 1991), implemented in a similar way as Bovy et al. (2016) and Braun and Willett (2013) on a regular grid. Sediments and water move from one cell to another using a steepest-descent algorithm. For each cell, a list of receivers (in other words cells that receive water or
210 sediment from another cell), r_s , are established by searching for the surrounding four neighboring cells that share an edge for a positive hydraulic gradient. The receiver cells and the positive hydraulic potentials are then stored in an array. For each cell, the positive hydraulic gradients are summed and divided by the number of receivers, n_r , to establish the weight or percentage of flow, w_r , to each receiver, using the array. The algorithm then uses the information about the number of receivers to determine the donor cells (in other words cells from which the given cell receives water or sediments), d_n . Note there can be several donor
215 cells, n_d , for each cell. Equipped with the information about the receivers and donors from each cell, the algorithm creates a stack s_t , a vector of cells ordered to perform operations.

These algorithms are encoded in a function,

$$s_t, r_s, n_r, w_r, n_d = \text{make_stack}(f_f).$$

The flotation fraction for a cell is calculated by $f_f = \frac{\phi}{\phi^*}$, where hydraulic potential ϕ comes from integrating Equation 1 up the stack to a cell and ϕ^* comes from determining the Shreve potential at overburden. We distribute the mean value of f_f across the glacier, then implement the routing scheme for the hydraulic potential determined from the Shreve potential. Here, we also assume that water does not inherit previous channels or canals (Figure 3; Shreve, 1972; Werder et al., 2013; Zechmann et al., 2020). The user can select whether the node ordering remains fixed for a given flotation fraction, f_f , over the model run or whether the node ordering evolves. We use a regular grid to discretize the bed. Spatial discretization must be substantially smaller than characteristic length-scale, l , in Equation 8. We then solve Equation 7 for till height H for given initial and boundary conditions in response to hydraulic forcing. In the model implementation we chose, the node ordering algorithm is executed every time step to account for diurnal variations in water pressure (e.g. Iken and Bindsehadler, 1986), which unavoidably increases simulation times. However, to improve stability during periods of rapidly changing sediment transport conditions, we reorder the stack, based upon the hydraulic conditions to the nearest 6. Smaller solving tolerances increase the computational time (Figure ?? e, f) due to 1) increased accuracy of the solution and 2) the reassessment of flow fractions between the adjacent cells, which results in different routing configurations as the model converges. We fill closed basins or over-deepenings in the hydraulic potential to maintain continuous sediment transport through the domain. The model uses an external algorithm, slightly modified, from the package *WhereTheWaterFlows.jl*¹ that contains flow routing and basin filling algorithms based upon rasterised DEM still production \dot{m}_t and divergence of the sediment discharge Q_s using an explicit time integration scheme.

2.3.2 Numerical implementation and parameter constraints

We discretize Equation 7 over the model domain space using a finite volume scheme on a regular grid. Spatial discretization must be substantially smaller than characteristic length, l , in Equation 7.

For the discretization in To discretize the problem in time, the model implements the VCABM solver (Hairer et al., 1992; Radhakrishnan and Hindmarsh, 1993) from the package *DifferentialEquations.jl* (Rackauckas and Nie, 2017) to evolve till layer height H . This solver implements an adaptive time step and uses a linear multi-step method (Adams-Moulton multistep method (Adams-Moulton)) that is well-suited for non-stiff problems, which is optimal because of the rapid fluctuations in sediment transport that can occur. We impose a maximum time step of 6 h to ensure that the model captures the response to diurnal variations in melt input. In practice, the solver commonly uses a time step of roughly 20 mn, which varies depending on sediment transport conditions and solver tolerance. Longer time steps occur over periods when glacier melt, and thus sediment transport, cease, such as winter months cease (i.e., winter months). Table 3 presents the numerical parameters used.

Benchmark experiments were conducted based upon the model setup discussed below in Section 3.1. Benchmark results show that the accuracy and performance of the model is optimized when solving tolerances (abstol, reltol, Table 3) are both on the order of 10^{-8} (Figure ??). Results also show that model behavior varies to a degree on grid-size due to the quantity of material in a grid cell and the flow of water through these cells (Figure ??, a,c).

We impose boundary conditions on the edge cells such that no sediment flux so no sediment enters the domain. At outlet cells, a flux of sediment leaves the domain, based upon on sediment transport conditions. Boundary conditions could also be

¹

set to represent processes such as ~~hill-slope~~hillslope erosion that route material to the subglacial environment (e.g. Andersen et al., 2015).

255 Evolving Equation 7 requires an initial till height, H_0 , ~~to be~~ chosen by the model user. This initial till height represents material from bedrock erosion created prior to the model initialization. We apply a “spin-up” procedure to create a reasonable relationship between the amount of fluvial sediment transport and bedrock erosion. ~~The amount of time needed to add material to the till layer means that an equilibrium between fluvial sediment transport and bedrock erosion will likely take centuries or longer to attain, if such a thing may even exist in light of variable climatic, and thus glacier, conditions. Should an equilibrium exist, it is probably outside a feasible computational time (Delaney and Adhikari, 2020). We consider this equilibrium (or lack thereof) and the implications of sediment storage in the subglacial environment an important research topic (e.g. Riihimaki et al., 2005; Otto et al., 2009), yet also one that is partially assessed in this manuscript.~~

260 ~~In addition to the initial condition, SUGSET contains 20 parameters that influence simulated physical processes in the model (Table 2 and 3). Subglacial hydrology models are well known to contain a large number of unconstrained parameters (e.g. de Fleurian et al., 2018). About half of these parameters are approximated in previous studies. Work in recent years has aimed to better evaluate these parameters through inverse methods (Brinkerhoff et al., 2016) as well as detailed modeling and measurements (e.g. Chen et al., 2018; Covington et al., 2020). Nonetheless, the situation leaves much to be desired.~~

New versions of the code are tested against reference ~~test~~ cases to ensure ~~that new versions remain consistent~~consistency. Additionally in each test, we ensure mass conservation by checking that the amount of sediment leaving the system through fluvial transport is consistent with the ~~till height~~till height change and erosion occurring under the simulated glacier.

270 3 **Model Application**

~~We present the model in three different applications that show its viability under increasingly complex situations. Two of the cases are synthetic scenarios based upon the Subglacial Hydrology Model Inter-comparison Project (SHMIP; de Fleurian et al., 2018), which provided a qualitative comparison of subglacial hydrology models using set of benchmark experiments. First, we apply the model with a synthetic ice sheet geometry with point inputs of water to~~

275 2.0.1 Routing algorithm and implementation

Sediment and water are routed down the hydraulic gradient using a multi-cell routing scheme (Quinn et al., 1991), implemented in a similar way as Bovy et al. (2016), but instead on a regular grid. Sediment and water moves from one cell to another using a steepest-descent algorithm, based upon the hydraulic potential. This routing scheme returns a stack, which contains information about the order of cells to perform the calculations. The model evaluates the hydraulic potential at every time step, first, the
280 flotation fraction for a cell at a given time is calculated by $f_f = \frac{\phi_o}{\phi_o^*}$, where hydraulic potential ϕ_o comes from

$$\phi_o = \phi_o + \sum_{j=1}^{n_r} \Psi_j \cdot \delta^{\frac{1}{2}} \cdot w_{r_j}. \quad (16)$$

Here, Ψ_j comes from Equation 1, δ is the area of a cell on a regular grid yielding cell length, n_r is the number of receivers that the cell has, and w_r is the proportion of hydraulic potential fed by the bed (moulins). This allows us to highlight the importance of evaluating water routing and sediment transport in two dimensions, even for the most simple glacier and bed geometries. Second, we apply the model to a synthetic alpine glacier, also based on SHMIP, to illustrate the model's performance in a more complex, realistic topography forced by a seasonally varying hydrology. Lastly, we apply the model to the topography, and sediment and water discharge at Griesgletscher in the Swiss Alps. We demonstrate the proficiency of the model by comparing sediment transport model output and data (Delaney et al., 2018a). We also identify some drivers of subglacial sediment discharge from these simulations.

285

2.1 Synthetic ice sheet test cases

290

2.0.1 Model parameterization and experiment design

We run synthetic ice sheet glacier experiment where the surface topography has a parabolic profile and bed topography remains flat. The spatial domain is 100 long and 20 wide. The identical geometry has been applied to the subglacial hydrology model presented in Werder et al. (2013) and SHMIP (de Fleurian et al., 2018). SHMIP also inspires the hydrology parameterization. Moulins route surface melt to the glacier bed as in Suite B4 of SHMIP (c.f. de Fleurian et al., 2018). Here, 50 moulins are distributed. We distribute the mean value of f_f across the glacier, with a greater concentration in the lower elevation sections of the glacier. The location of these moulins can be found in the code repository or at the SHMIP website¹.

295

To summarize the hydrology parameterization presented in Suite B4 of SHMIP, the meltwater source term, \dot{m}_w , is defined as,

$$\dot{m}_w(z_s) = \begin{cases} M_f T(z_s) & \text{if } T(z_s) > 0 \\ 0 & \text{if } T(z_s) \leq 0 \end{cases}$$

300

and then implement the routing scheme for the hydraulic potential determined from the Shreve potential as

$$\phi = f_f \rho_i g (z_s - z_b) + \rho_w g z_b. \quad (17)$$

where $M_f = 0.01$

The node ordering algorithm is executed every time step in response to diurnal variations in water pressure and thus variable routing of subglacial water in response to changing hydraulic conditions (e.g. Iken and Bindschadler, 1986; Chu et al., 2016). However, to improve stability during periods of rapidly changing sediment transport conditions, we reorder the stack, based upon the hydraulic conditions to the nearest $6 \text{ m K}^{-1} \text{ d}^{-1}$ is a melt factor, and $T(z_s)$ is air temperature at elevation z_s .

305

$$T(z_s) = \left(A_d \cos \left(\frac{2\pi t}{s_{day}} \right) + \Delta T \right) \cdot \left(1 + z_s \frac{dT}{dz} \right),$$

¹

A_d is the diurnal amplitude in temperature, ΔT is a temperature offset that is adjusted to control the meltwater input and s_{day} is the number of seconds in one day. In these simulations, melt varies diurnally, but not seasonally.

310 We then apply Equation 20 to cells for which a moulin exists to localize the water source, however, ΔT is greatly increased so that the model produces realistic values of water discharge^{mm}. Smaller solving tolerances increase the computational time due to 1) increased accuracy of the solution and 2) the reassessment of flow fractions between the adjacent cells, which results in different routing configurations as the model converges. We fill closed basins in hydraulic potential to maintain continuous sediment transport through the domain. The model uses an external algorithm, that contains routes flow and fills basins based upon rasterised values of the hydraulic potential.

315 Here, we adjust the parameterization of erosion such that the glacier uniformly creates 3^{-1} of till across the bed, replacing Equation 15 with Using this routing scheme, we are able to evaluate the water discharge in a cell from melt upstream as

$$Q_w = \frac{0.003}{s_{year}} \dot{m}_w \cdot \delta + \sum_{j=1}^{n_r} Q_{w_j} \cdot w_{r_j}, \quad (18)$$

320 such that \dot{m}_r still depends on till height H (Equation 12). s_{year} represents where \dot{m}_w is a melt water source term and n_r is the number of seconds in a year.

We run the model using only a diurnal hydrology forcing. For the first 10 a steady forcing of ΔT is applied. After 10, ΔT is increased 1.5° every year for 10 then run for another 10, such that total model run time is 30. The model run initiates with 5 of till at the bed, the limit of till grown (H_{max} Equation 12). Quantities of sediment below glaciers remain generally unknown and may be quite substantial (e.g. Truffer et al., 2000). We chose 5 as an initial condition as we predict that it captures erosion processes on the millennium timescales, given erosion rates of $1-3^{-1}$ (Hallet et al., 1996). receivers of that cell. The sediment discharge Q_s into a cell is like-wise computed as

$$Q_s = \sum_{j=1}^{n_r} Q_s \cdot w_{r_j}. \quad (19)$$

A spin-up is conducted over the initial hydrological conditions until the annual erosion rate reaches 10^{-4}^{-1} . We believe this spin-up sets the conditions for quantifying hourly sediment transport in light of the millenia scale quantities of bedrock erosion, that represent our initial condition.

330 2.0.1 Model outputs and findings

Over the course of the model run, water discharge increases roughly 10% between year 10 and year 20. Over the corresponding period, sediment discharge increases to roughly 2% from the pre-perturbation values of sediment discharge. At the same time, the general trend of increasing till height persists through the climate forcing, although at a slower rate (Figure ?? a). Sediment transport capacity, Q_{sc} lies at over 10 times sediment discharge.

335 In our simulations, sediment transport occurs in a very limited portion of the glacier bed, where the water flows. Thus
till height remains consistent through the model run across the vast majority of the domain (Figure ??). At the same time,
even this localized water flow and sediment transport produces catchment erosion rates of roughly 1 m^{-1} , which is on the
order of some measured erosion rates from the Greenland Ice Sheet (Cowton et al., 2012; Overeem et al., 2017), but also in
mountainous regions (Hallet et al., 1996).

340 Sediment discharge in the model run decreases after the climate warms and reaches a stable regime. The decrease occurs
due to sediment exhaustion from increased water discharge, and thus sediment transport, which removed till that was unable
to be transported in a cooler climate with less available meltwater able to transport sediment.

We note that till height along certain channels is discontinuous, and the till height increases from where the water enters
the glacier through a moulin to the terminus (Figure ??). At a certain distance from the moulin (roughly 2 in this case),
345 subglacial water attains its transport capacity and cannot mobilize additional sediment at Q_s is then used to evaluate the $\nabla \cdot Q_s$
given Equation 8 and subsequently, the change in till height using Equation 7. In both Equation 18 and 19, the operations
are conducted given the node ordering information in the same rate as higher on the glacier. We note that due to sediment
exhaustion these features are transient, and their persistence, location and size will respond to the sediment source term (\dot{m}_t)
and the sediment e-folding length (l). These bare bedrock patches serve as a source of sediment that is in part responsible for
350 the increase in sediment discharge after the climate forcing at the end of the model run (Figure ??). stack, such that the flux in
to a cell depends on the flux through the catchment above it.

Given our routing parameterization and the laterally consistent geometry of the glacier, this test case essentially represents
many one-dimensional models set up in parallel, as each cell has a single receiver cell. Yet, even in this simple case, collapsing
the problem to a single dimension means that sediment thickness will either be averaged over the entire glacier width, or that
355 only a single moulin or water source can be considered. In light of these experiments, we suggest that in most applications where
the researcher's interest lies in sediment discharge, two-dimensional consideration of sediment dynamics more adequately
captures relevant processes than a one-dimensional framework

3 Model Application

360 We use two cases to highlight model viability under increasingly complex situations. First, we apply the model to a synthetic
alpine glacier with synthetic hydrology, based on the Subglacial Hydrology Model Inter-comparison Project (SHMIP; de Fleurian et al., 20
, to illustrate the model's performance in a simplistic scenario. We then apply the model to the topography, and sediment and
water discharge at Griesgletscher in the Swiss Alps. We demonstrate the proficiency of the model by comparing sediment
transport model output and data (Delaney et al., 2018a). We also identify some drivers of subglacial sediment discharge in the
model from these simulations.

3.1.1 ~~Model parameterization and experiment~~ Experiment design

We run simulations using an alpine glacier geometry and hydrological forcing following the SHMIP project experiments (de Fleurian et al., 2018). The domain is 6000 m on one axis and 1080 m on the other ~~and the~~. The resulting geometry approximates the Bench Glacier. The ~~U-shaping~~ U-shaped bed and variable ~~ice-sheet~~ ice thickness mean that variable hydrologic
 370 gradients will occur laterally across the glacier and water can be routed across ~~multiple cells, unlike the ice sheet case from~~ ~~Section ??~~ multiple cells.

To ~~parameterize~~ represent hydrology, we ~~return to the melt model in Equation 20~~. Temperature ~~implement a simple melt~~ model as in SHMIP (de Fleurian et al., 2018)

$$\dot{m}_w(z_s) = \begin{cases} M_f T(z_s) & \text{if } T(z_s) > 0 \\ 0 & \text{if } T(z_s) \leq 0 \end{cases}, \quad (20)$$

375 where $M_f = 0.01 \text{ m K}^{-1} \text{ d}^{-1}$ is a melt factor. $T(z_s)$ is air temperature T at elevation z_s ~~for this test case is~~ defined as

$$T(z_s) = \left(-A_a \cos\left(\frac{2\pi t}{s_{year}}\right) + A_d \cos\left(\frac{2\pi t}{s_{day}}\right) + \Delta T - 5 \right) \cdot \left(1 + z_s \frac{dT}{dz} \right), \quad (21)$$

where A_a and A_d are the annual and diurnal amplitudes, respectively, ΔT is a temperature offset, which is adjusted to control the meltwater input and s_{day} are the number of seconds in one day, s_{year} is the number of seconds in a year and $\frac{dT}{dz} = -0.0075 \text{ K m}^{-1}$ is the air temperature lapse rate. In this ~~test~~ case, we route water directly to the ~~glacier bed~~ subglacial system
 380 at the location where the melt occurs, ignoring moulins that concentrate meltwater delivery to the bed.

~~Similar to the ice sheet case (Section ??), we~~ We run the model for 12 years with a steady climate ~~forcing~~, then we apply a ~~gradual climate forcing~~ linear temperature increase for 8 years followed by 10 years of steady ~~climate forcing~~ temperature at the maximal ΔT . The ~~annual temperature signal experiences randomly distributed noise to mimic the effects of inter-annual variability~~ model is initiated with 10 cm of till across the bed. A spin-up over one year of the initial hydrological forcing is
 385 applied ~~until either for~~ 150 a ~~is reached~~ or an annual change in the till layer height is less than $10^{-4} \text{ mm a}^{-1}$, ~~i.e.~~, well below the annual erosion rate in most glacierized catchments (Hallet et al., 1996).

3.1.2 Model outputs and findings

~~Model outputs~~ Simulations show that over seasonal timescales, sediment discharge increases at the onset of melt and decreases shortly thereafter, prior to the maximum amount of water discharge that occurs each melt season (Figure 4). Daily-averaged
 390 sediment discharge decreases until the very end of the melt season when sediment discharge increases slightly again (Figure 6). This occurs when water stops flowing during the night ~~and sediment may~~ allowing sediment to accumulate in the channels from bedrock erosion. Increased sediment discharge at the beginning of the melt season results from greater sediment availability

following the growth of the till layer over the winter months, when ~~little water is available for sediment transport~~ the small amount of melt limits transport sediment.

395 Increases in sediment discharge at the onset of melt ~~and subsequent exhaustion of sediment have been documented in field observations~~ have been observed for real glaciers (Willis et al., 1996; Swift et al., 2005; Riihimaki et al., 2005; Delaney et al., 2018b) and reproduced in the one-dimensional version of this model (Delaney et al., 2019). However, in SUGSET_2D, larger diurnal increases in sediment discharge occur ~~because water only accesses certain patches of the glacier bed for a limited time during the diurnal cycle. This transient flow maintains the till layer there, allowing it to even grow slightly from bedrock erosion.~~
400 ~~The temporal variability in meltwater access to portions~~ near peak daily melt because the area of flowing water expands under the glacier. As a result, increased sediment transport may occur in cells with substantial sediment when hydraulic conditions permit, then abandoned them when water is routed to another part of the glacier bed ~~lies contrary to the~~. This allows sediment to be stored in these cells, until the hydraulic conditions return and increased sediment transport may return. Such a process is difficult to represent in a one-dimensional model, where ~~meltwater access to the glacier bed is only limited along the glacier's~~
405 ~~longitudethe many of the cells could be represented together.~~

Over the course of the ~~model runsimulation~~, the mean ~~till height continues to decrease over annual scales, till height decreases and more sediment is expelled from the glacier as the system adjusts to the change in climate (Figure 5). This occurs~~ despite the spin-up threshold of 10^{-4} mm a⁻¹ change in till height per year, highlighting the difficulty in ~~evaluating an achieving a true~~ equilibrium between bedrock erosion and sediment transport (Figure 4,c). ~~However, till height~~ Till height
410 ~~decrease accelerates following the onset of increased melt at year 12. Over the same periods, annual amounts of sediment discharge increased due to decreased subglacial sediment storage (Figure 5). When a~~ With the new steady climate was reached at year 20, ~~the~~ annual quantities of sediment discharge began to decrease. ~~This occurs~~ as the system ~~approached a new equilibrium~~ approaches a stable relationship between sediment transport and bedrock erosion. ~~This process also occurred in the ice sheet test case (Section ??).~~

415 Interestingly, the model recreates "first-flush" events of increased sediment discharge early in the melt season (Figure 6), followed by decreased sediment discharge (Swift et al., 2005; Delaney et al., 2018b). This seasonal evolution in sediment discharge ~~has been is~~ attributed to increased access to subglacial sediment early in the season, followed by decreased access ~~to sediment when the flow is as~~ flow becomes increasingly channelized (e.g. Willis et al., 1996; Swift et al., 2005). ~~In a warmer climate, seasonal~~ As melt begins in the spring, sediment discharge increases, largely due to increased sediment transport high
420 on the glacier (Figure 4). However, ~~seasonal~~ maximum values of sediment discharge during "first-flush" ~~event events~~ decrease because sediment transport also occurs over that time. ~~Winter sediment transport prevents~~ By the end of the simulation, winter transport is large enough to prevent the till layer from growing ~~over the winter months, creating a surplus of sediment to be transport in the spring. While this model output could be considered interesting, we note. This maintains a sediment reservoir available for transit when melt increases. Note~~ that the model does not couple ice dynamics to ~~the~~ sub-glacial hydrology, so
425 erosive potential, water discharge and ~~the~~ subglacial area will ~~likely~~ decrease as well in response to the ~~new climate. The increase could also occur with increased~~ changing climate. Additionally, increased subglacial water discharge could enhance sliding, and thus erosion, ~~following melt~~ may occur following the onset of melt in the spring (Ugelvig et al., 2018).

For the ~~test cases~~ cases described above, bedrock erosion ~~essentially relied~~ relies only on driving stress and ~~thus sliding and bedrock erosion till thickness~~. Sliding and bedrock erosion did not vary seasonally ~~, except for limits on sediment production with till layer height~~ (Figure 6 a, b, Section 3.1). This causes ~~a buildup of sediment~~ sediment to accumulate during the winter months, which subsequently ~~provided~~ provides ample material for transport when melt increases in the spring. The model's bedrock erosion scheme is likely valid on most applicable to land-terminating glaciers and over long-time scales when driving stress ~~exerts the~~ likely exerts a primary control on glacier sliding (~~e.g. Weertman, 1957~~) (e.g. Weertman, 1957; Gimbert et al., 2021). However, by coupling subglacial hydrology to erosion Ugelvig et al. (2018) ~~showed~~ shows that erosion varies seasonally and abrasion largely occurs solely during the summer months. Additionally, in the ~~test~~ case presented above, sediment production ~~occurred~~ occurs primarily near the glacier front, where ~~ice deformation~~ driving stress, and thus sliding, is ~~greatest~~ highest (Figure 3, a).

To test the effects of spatially variable erosion and the role of hydrology, we present two additional ~~test~~ cases to supplement the alpine glacier ~~test~~ case above, *ORIGINAL*.

~~The first test~~ The first case, *SEASON*, simulates bedrock erosion by increasing sliding during the summer months (e.g. Iken and Bindschadler, 1986), the same erosion relationship is applied as the case as Section 3.1. ~~In this case~~ however, erosion only occurs when the amount of water input substantially exceeds the ~~basal melt rate~~ background basal melt input rate, that is present in the winter. In the second ~~test~~ case, *CONST*, bedrock erosion remains constant over the entirety of the glacier at a rate of 1 mm a^{-1} .

The *ORIGINAL* ~~test~~ case discharges over ~~4650~~ 11620 m^3 of sediment per year, while the *SEASON* case discharged only 60% of that value due to the absence of bedrock erosion during the winter months. The *CONST* case discharged ~~2160~~ 7320 m^3 of sediment over the year. ~~This value is substantially less than the~~ CONST's quantity of sediment discharge results in roughly 1 mm a^{-1} erosion rate due to decreased erosion efficiency with till height (Equation 12 and the limited portion of the bed over-which sediment transport occurs (Figure 5).

Over the three cases, sediment discharge increases at the onset of melt and substantially decreases by the end of the melt season due to sediment exhaustion. In *ORIGINAL* (Figure 6 a, b), more sediment discharge occurs compared to the alternate ~~test~~ cases (*SEASON* and ~~both~~ CONST). The increased sediment discharge in ORIGINAL is due 1) to the prolonged period over which bedrock erosion occurs adding more sediment to the layer and 2) that bedrock erosion occurs low on the glacier where much sediment transport takes place, compared to the *CONST* case. The peak sediment discharge in *CONST* (Figure 6 e, f) occurs slightly earlier in the season, due to the increased amounts of sediment on the lower glacier margins.

3.2 Griesgletscher

3.2.1 ~~Model parameterization and experiment~~ Experiment design

~~Lastly, we apply the model to the~~ We also simulate Griesgletscher in the Swiss Alps using topographic data from (Delaney et al., 2019). Hourly water discharge from the glacier was modeled in Delaney et al. (2018a). Here, we use the discharge time series from 2009–2017. Subglacial sediment discharge from the glacier was determined for four different time periods since

fall 2011 by differencing ~~repeated~~ bathymetry maps (Delaney et al., 2018a). To ~~distribute glacier estimate surface~~ melt across the glacier with respect to elevation, we use,

$$\dot{m}_w(x, y) = \dot{b}^0 + \gamma(z_s(x, y) - z_s^0). \quad (22)$$

465 γ is the mass balance gradient and z_s^0 represents the glacier's lowest elevation. \dot{b}^0 represents the melt rate at the glacier's lowest extent. \dot{b}^0 was evaluated numerically at each water discharge value using the hypsometry of the glacier.

We apply a parameter search over a range of values of sediment ~~grain-size~~ grain size (D_m ; a primary control on fluvial transport of subglacial sediment), sliding ~~velocity~~ (~~f_{st}~~ rate factor (B ; a control on bedrock erosion), and the initial till height condition (H_0 ; to approximate the effects of existing quantities of sediment below the glacier). 100 ~~model runs were executed~~ simulations were run with randomly selected parameters from a uniform distribution. No spin-up was applied in this test case,
470 because of ~~computational expense and~~ the wide range of H_0 values explored.

The wall time for a single model run averaged 8.9 h, and each run for a parameter set was executed on a single CPU. Instead of applying the mean flotation fraction across the glacier, as was done in the previous ~~test~~-cases, the maximum value was applied with an upper limit of 1.

~~Only~~ We only considered model outputs resulting in a perfect rank correlation across the four data collection periods and an
475 error less than ~~85,000~~ 80,000 m^{-3} ~~were considered~~. For the ~~test~~-case presented below ~~we only~~, we show the simulation with the lowest absolute error between model output and the sediment transport data.

3.2.2 Model outputs and findings

The model ~~successfully captured the inter-annual~~ reproduces the interannual variability in sediment discharge from the Griesgletscher. The absolute error between the model and the measurements is roughly ~~62,477~~ 62,600 m^3 . The model ~~captures~~
480 represents the last three ~~time-spans very~~ measured yearly sums of sediment discharge well, but it has trouble reconciling the ~~increased~~ elevated sediment discharge in 2012 and 2013 (Figure 7). This suggests that processes not ~~included~~ adequately represented in the model are responsible for the increase in sediment transport, such as activation of new patches of the glacier bed or the relocation of channels (e.g. Zechmann et al., 2020), potentially due to changes to glacier surface topography that cause alternative flow paths below the glacier. Furthermore, ~~sliding parameter~~ f_{st} glacier sliding, remains constant over the
485 model run ~~in the absence of glacier velocity data~~, in turn, ~~inter-annual~~ the results do not explicitly account for seasonal or interannual variability in bedrock erosion ~~is not considered~~ (Herman et al., 2015)(e.g. Herman et al., 2015).

The error from this parameter search is slightly less than half of the 131,300 m^3 total sediment discharged from the Griesgletscher over this time period (Delaney et al., 2018a), and the error is slightly more than the 58,300 m^3 from the best model run of the one-dimensional model ~~(e.f. Delaney et al., 2019)~~ in Delaney et al. (2019). However, in contrast to the ensemble model
490 runs in Delaney et al. (2019), this model's ability to reproduce the validation data largely depends on the ~~grain-size~~ grain size parameter, D_m . Compared to Delaney et al. (2019), the sliding ~~fraction~~ parameters and initial condition parameters (~~f_{st}~~ B and H_0) have a minimal influence here when tuned to the data ~~here~~ Figure 7. ~~This is due to~~ The dependence on grain size

for ~~SUGSET_2D results from~~ the subglacial sediment connectivity parameterized in this ~~two-dimensional~~ ~~two-dimensional~~ version of the model. ~~In SUGSET_2D, the~~ ~~The~~ channelized nature of flow means that sediment transport may only occur over
495 a relatively narrow patch of the glacier bed (Figure 9). As sediment ~~grain-size~~ ~~grain size~~ decreases, sediment from locations of the glacier bed with ~~relative~~ ~~relatively~~ small water velocity and discharge can more easily be transported to the main glacier channel and be expelled from the glacier. In a one-dimensional model, sediment access occurs over the entire ~~glacier bed for a given elevation bandwidth of the glacier bed~~. Thus, the bedrock erosion or sediment production term (largely controlled by ~~f_{st}~~ ~~sliding rate factor B~~) represents this process, and increased sediment production results in greater connectivity.

500 The size and shape of the subglacial channels ~~contributes~~ ~~contribute~~ to the discharge of sediment, as well. The sediment transport due to the velocity of subglacial water is limited by the channel width in smaller channels (w_c , Equation 10). For this reason, sediment exhaustion occurs mainly in ~~localized~~ ~~main~~ channels, where channel widths are sufficiently large to allow substantial sediment transport (Figure 3). Conversely, sediment persists in patches of the glacier bed where ~~water~~ velocity could be high, but insufficient ~~channel-size~~ ~~channel size~~ effectively reduces sediment transport capacity. ~~Experience with tuning the model to the available dataset shows that increasing~~ ~~Increasing the~~ friction factor f_i increases the area of the glacier bed over-
505 which water with substantial velocity flows ~~in SUGSET_2D~~. Thus the model has trouble capturing ~~inter-annual~~ ~~interannual~~ variability because sediment exhaustion does not occur over a substantial portion of the glacier bed.

~~Smaller, and probably more realistic, values of f_{st} represent the data in SUGSET compared to SUGSET_2D (0.36 and 4.09, respectively)~~ ~~The value of B , from the parameter search, results in a average of 39 m a⁻¹ of glacier sliding across the glacier bed, and the range of values for B in the parameter search result in mean sliding velocities between 14 ma⁻¹ and 70 ma⁻¹.~~
510 Yet, ~~because of~~ ~~due to~~ the low dependence ~~on f_{st} , smaller of~~ ~~sediment transport from the glacier on B , other~~ values could perform well, ~~but not be~~ ~~but are not~~ captured in the relatively small number of model runs herein. ~~However, because sediment production decreases with~~ ~~till-height~~ ~~till height~~ (Equation 12), sediment production is limited to the narrow patches of the glacier bed where minimal till persists and bedrock erosion may occur. As a result, the model requires more sliding to produce
515 the equivalent amount of sediment, ~~even though the sliding and erosion parameters applied here are within a well constrained range~~. At the same time, the limited spatial extent of glacier erosion and sediment transport points to a need ~~, beyond this manuscript,~~ to evaluate the precise location of bedrock erosion and the impact of subglacial till layers on bedrock erosion ~~in future research~~.

The best performing model run shows strong temporal variability in sediment discharge (Figure 8), with water discharges
520 from the glacier above roughly $2 \text{ m}^3 \text{ s}^{-1}$ responsible for much of the sediment transport. Despite the strong dependence on ~~grain-size~~ ~~grain size~~ and fluvial transport of sediment in the inversion, sediment transport capacity Q_{sc} remains roughly an order of magnitude higher than sediment discharge (Q_{sc}). ~~A~~ ~~The~~ steep section of the glacier experiences sediment depletion over the model run, as do several channels near the over-deepening and high on the glacier (Figure 9 c d). ~~Several of areas surrounding the depleted areas show signs of deposition.~~ On some parts of the upper glacier, bedrock erosion in the absence
525 of substantial sediment transport is visible. With changing melt patterns or evolving glacier hydraulic gradients, this sediment could be mobilized and increase sediment discharge down glacier.

4 Model limitations

530 The lack of knowledge regarding the spatial distribution of subglacial sediment makes selecting an initial value of H difficult. The slow rate of basal erosion means that an equilibrium between fluvial sediment transport and bedrock erosion will likely take centuries to attain, if such an equilibrium may even exist in light of variable climatic, and thus glacier, conditions. Should an equilibrium exist, it is probably outside of a feasible computational time given current processing speeds (e.g. Herman et al., 2018; Delaney

~
In addition to selecting an initial value of H , we also limit the thickness at which the till must stop accumulating (Equation 8b, H_{lim}) due to changes in the hydraulic potential caused by channel infill. We assume that this value is on the order of
535 tens of centimeters (Table 2), based upon available observations (Perolo et al., 2018). While the impact of a till-layer on bedrock abrasion remains uncertain, we expect that sediment of a certain thickness will armor the bed preventing erosion (Alley et al., 2003). In turn, we limit erosion with till thickness to a threshold (5 cm), on the same order of H_{lim} to improve computational time. Additionally, the model does not consider the interactions between fluvial transport of sediment and debris concentrations in subglacial ice, which may be important for sub-glacial sediment transport (e.g. Ugelvig and Egholm, 2018).

540 SUGSET_2D also contains 20 parameters (Table 2 and 3). These parameters have only been partially constrained using inverse methods (Brinkerhoff et al., 2016) as well as detailed modeling and measurements (e.g. Chen et al., 2018; Covington et al., 2020; P

~
The routing method we use assumes that water solely flows in response to the hydraulic potential (Section 2.0.1). Our
545 parameterization does include the impact of a channel's size on the hydraulic potential. It also does not explicitly simulate the evolution of efficient and inefficient subglacial drainage systems over the course of the season, or the inheritance of existing subglacial canals or channels (Figure 3; e.g. Werder et al., 2013; Zechmann et al., 2020). Furthermore, a response time of the subglacial channel is chosen prior to simulations to improve computational time, compared to a more sophisticated representation or processes in an R-channel (e.g. Röthlisberger, 1972).

5 Implications

550 Results of both the one-dimensional model (SUGSET; Delaney et al., 2019) and SUGSET_2D highlight the importance
~~parameterizing of simulating~~ the spatial heterogeneities in bedrock erosion, sediment availability, and sediment transport capacity. Yet, in ~~the one-dimensional model SUGSET~~, only the ~~limits in the till-layer model till layer~~ (e.g. Equation 8c) and variations in sediment access along the glacier flow line impact sediment ~~mobilization. In the two-dimensional model here~~ transport.
555 In SUGSET_2D, sediment access and transport is not averaged over the glacier width. Rather, by considering the spatial distribution in water discharge and sediment availability laterally below a glacier, the model evaluates where heterogeneities may persist and their impact on subglacial sediment dynamics (Figures ~~??~~, 5, and 9).

~~In the context of an ice-sheet-like glacier where moulin inputs localize water flow, this means that in a one-dimensional model, the spatial area below the glacier over which water from a moulin can transport sediment will be dramatically over-estimated (Section ??). The model here fails to account for the seasonal evolution in water routing from a distributed to channelized~~

560 drainage system (e.g. Werder et al., 2013). Even so, the localization of water flow means that sediment transport may often occur in a supply-limited regime and thus bedrock erosion or input of sediment into the channel figures strongly in to sediment discharge (Figures ?? and ??). Should this model's characteristics hold true in the natural environment, then it may well explain why a glacier's erosion potential might be a stronger control on sediment discharge from the Greenland Ice Sheet compared to water discharge (Overeem et al., 2017).

565 Subglacial drainage below the Greenland Ice Sheet in response to climate warming remains highly uncertain, and the evolution of subglacial channels largely depends on the locations where meltwater reaches the glacier bed (Poinar et al., 2015; Gagliardini et al., 2015). The experiments presented here suggest that rising temperatures and increased glacier melt may result in greater sediment transport from ice sheets (e.g. Bendixen et al., 2017) by accelerating sediment mobilization in regions of the bed where mobilization was reduced before. We note though, that the simulations presented here did not account for changes in ice sheet thickness and velocity following glacier melt (e.g. Sundal et al., 2011; Tedstone et al., 2015; Mouginito et al., 2019). Such changes will certainly impact bedrock erosion (e.g. Herman et al., 2021). Additionally, changes to topography and relatively lower hydraulic gradients on the ice sheet may well reroute subglacial water (Chu et al., 2016), and in the processes, new subglacial sediment sources might be accessed and reached. Given the prolonged increase anticipated melt (e.g. Aschwanden et al., 2019), sediment transport and bedrock erosion are unlikely to trend toward a new equilibrium, as they do after the model reaches a new climate (Figure ??).

575 The large Large diurnal and seasonal fluctuations in sediment transport at in the synthetic alpine glacier case result from diurnal and seasonal variations in water routing and thus increased sediment availability because sediment transport only occurs over a patch of bed for a short amount of time (Section 3.1). For instance here, diurnal fluctuations in sediment discharge in the middle of the season can be over to 50% above the mean value, which aligns more closely with some field observation of sediment discharge (e.g. Swift et al., 2005; Delaney et al., 2018b) compared to the one-dimensional model SUGSET (c.f. Delaney et al., 2019). Furthermore, the results show that the location of bedrock erosion, processes in the till-layer, and the timing of melt all play an important role in the quantity of sediment discharge and the peak sediment discharge that is reached.

In the final test case, we compared model runs across a parameter space to sediment discharge data from Griesgletscher in the Swiss Alps (Section 3.2). These results depended solely on sediment grain size compared to the initial till condition or bedrock erosion (Figure 7). The model's strong dependence on grain size in capturing data is caused by the transport of sediment from patches of the glacier bed with slow water velocity or channel cross-sectional area to the larger, main channels Grain size is a strong control in the SUGSET 2D because it modulates how easily sediment patches only accessed by sub-glacial flow during the melt season are mobilized. This process could not cannot be considered in a one-dimensional model, though it appears quite important at is important even in this relatively small and shallow glacier. Yet, these results suggest alpine glacier. These results show that connectivity between the distal patches of the glacier bed and predominant channels flowing below the glacier remain highly important for the quantity of sediment discharge. This process subglacial channels and distal sediment patches is a strong control on sediment discharge from the subglacial system. The connectivity between the main channels and distal sources of sediment could be through the transport of small sediments as applied here or but could conceivably, but may also occur through other processes not considered in the model, such as till deformation (e.g. Damsgaard et al., 2020). In these locations, slightly

595 ~~lower water velocities and reduced channel width for sediment mobilization to occur limit the amount of sediment mobilization that occurs. Limited measurements bedload measurements suggest that suspended sediment, as opposed to bedload, comprises the majority of sediment leaving glaciers (Riihimaki et al., 2005; Geilhausen et al., 2013; Delaney et al., 2018b). The model here does not differentiate between bedload and suspended sediment transport, yet water access to sediment contributes substantially to~~

600 ~~Lastly, the export of suspended sediment, compared to bedload transport. Meltwater access to~~ model demonstrates the complex nature of subglacial sediment transport and the transitions between supply- and transport- limited regimes. Sediment discharge depends not only on hydrology but also on the sediment is a process that SUGSET_2D represents, which is also an evidently important process in sediment discharge from glaciers availability. Equivalent values of water input and sediment transport capacity below the glacier result in simulated sediment discharge that vary over orders of magnitude (Figure 10, a).
605 In turn, using solely the water discharge or sediment transport capacity (e.g. Equation 10) fails to consider the changes to sediment availability caused by sediment transport, especially when changes to sediment storage can take place over seasons to decades. Finding ways to evaluate these difficult to measure parameters could be key to improving our understanding of subglacial sediment transport.

6 Conclusions

610 This manuscript presents a two-dimensional subglacial sediment transport model, SUGSET_2D, that evolves a till-layer in response to subglacial ~~sediment transport conditions. Model test hydrology. Model~~ cases utilize geometries and hydrological forcings from a synthetic ~~ice sheet, synthetic alpine glacier, and real and a real alpine~~ glacier. The model captures sediment transport in supply- and transport- limited regimes ~~and conserves mass in the till-layer~~. Results from ~~each test case both cases~~ point to the need to quantify the spatial distribution of subglacial sediment and water when ~~determining sediment discharge from the subglacial environment. Furthermore, outputs align with some observed sediment dynamics~~ simulating sediment discharge expelled from glaciers. Model outputs reproduce many observed subglacial sediment processes.

Despite the model's ~~capabilities, it contains ability to reproduce observations, it relies on~~ a large number of poorly constrained parameters. ~~Furthermore, to~~ To our knowledge, ~~the only one study quantified the thickness of till below a glacier, and this value was a single point measurement (Truffer et al., 2000). As a result, in the absence of this knowledge, prescribing initial till height conditions must be done in a thoughtful manner that considers the hysteresis in the till layer stemming from~~ has quantified till thickness at a single point below a glacier (Truffer et al., 2000). These observations are limited due to the difficulty of making direct observations at glacier beds. The initial till height in the model must be chosen carefully because the system can remember this initial condition for centuries. The interaction of bedrock erosion and fluvial sediment transport
~~Depending on research questions, two-dimensional models may provide the most robust outcomes when operated across a parameter space and in concert with available observations of erosion or sediment transport. Additionally, the method to route subglacial water at glaciers with complex geometry must be carefully evaluated. Here, we route also leads hysteresis in the system.~~
625 system.

Two-dimensional sediment transport models can represent more observed characteristics of subglacial sediment discharge compared to one-dimensional models. SUGSET 2D routes water and sediment based-up-using the Shreve potential by-using and a spatially uniform flotation-fraction that evolves temporally-in time in the real glacier case (e.g. Section 3.2). Future work may consider using a coupled model of channelized and distributed drainage networks (Hewitt et al., 2012; Werder et al., 2013) -(Hewitt, 2013; Werder et al., 2013). Increasing the sophistication of the subglacial hydrology model may better evaluate the locations of high potential sediment transport. Such models could even be run offline if the operator assumes, as we do, that rates of change in till height remain-are small compared to the evolution in cross-section of the subglacial conduit.

630 ~~Model-outputs~~ Our simulations highlight that increased glacier melt ~~do~~ does not necessarily result in ~~proportional-commensurate~~ changes to sediment discharge ~~if new subglacial sediment sources are not accessed~~ unless new previously inaccessible subglacial sediment patches are accessed by meltwater. Additionally, results demonstrate the role of spatially varying water routing and lateral sediment connectivity in subglacial sediment discharge. ~~In our opinion, among the most important topics regarding glacier erosion lies in assessing the response time of glacial~~ Further efforts should constrain the role of climate change on glacial

640 ~~dynamics,~~ erosion and sediment transport ~~to changes in glacier dynamics. Hopefully modeling work, such as this,~~ Further modeling and observational studies ~~will help to better understand the time-scales~~ are needed to better constrain the timescales over-which these ~~respective processes occur and their~~ processes occur in response to climate ~~and glacier dynamics~~ change.

Code availability. The code library along with illustrative examples are available at <https://bitbucket.org/IanDelaney/sugset.jl/src/id-2d>. The running and plotting scripts used in the cases herein are stored at https://bitbucket.org/IanDelaney/2d_runners/src/master/.

645 *Video supplement.* Videos of a prior model version's application to Griesgletcher are available at <https://bit.ly/3nPvVUI>, demonstrating model behavior. Similar videos of the current model version will be transferred to a permanent location pending acceptance.

Author contributions. ID designed the study, developed the model, ran the cases and lead writing the manuscript. LA assisted with the writing the manuscript and provided key advice designing and troubleshooting the model. FH provided guidance with implementing and designing the model and preparing the manuscript.

650 *Competing interests.* The authors declare no competing interests.

Acknowledgements. We thank J. Braun, B. Bovy, F. De Doncker, S. N. Lane, G. [Jouvet, G.](#) Prasicsek and M. Werder for fruitful discussions and insightful comments. We are also grateful to Grégoire Mariéthoz and the Scientific Computing and Research Support Unit at Université

de Lausanne for providing computing resources. I. Overeem, S. Hergarten and an anonymous reviewer provided thoughtful and constructive comments that greatly improved this manuscript.

655 **References**

- Alley, R. B., Cuffey, K. M., Evenson, E. B., Strasser, J. C., Lawson, D. E., and Larson, G. J.: How glaciers entrain and transport basal sediment: physical constraints, *Quaternary Science Reviews*, 16, 1017–1038, [https://doi.org/10.1016/S0277-3791\(97\)00034-6](https://doi.org/10.1016/S0277-3791(97)00034-6), 1997.
- Alley, R. B., Lawson, D. E., Larson, G. J., Evenson, E. B., and Baker, G. S.: Stabilizing feedbacks in glacier-bed erosion, *Nature*, 424, 758–760, <https://doi.org/10.1038/nature01839>, 2003.
- 660 Andersen, J. L., Egholm, D. L., Knudsen, M. F., Jansen, J. D., and Nielsen, S. B.: The periglacial engine of mountain erosion– Part 1: Rates of frost cracking and frost creep, *Earth Surface Dynamics*, 3, 447–462, <https://doi.org/10.5194/esurf-3-447-2015>, <https://esurf.copernicus.org/articles/3/447/2015/>, 2015.
- Aschwanden, A., Fahnstock, M., Truffer, M., Brinkerhoff, D., Hock, R., Khroulev, C., Mottram, R., and Khan, S. A.: Contribution of the Greenland Ice Sheet to sea level over the next millennium, *Science Advances*, 5, <https://doi.org/10.1126/sciadv.aav9396>, 2019.
- 665 Beaud, F., Flowers, G., and Venditti, J. G.: Modeling sediment transport in ice-walled subglacial channels and its implications for esker formation and pro-glacial sediment yields, *Journal of Geophysical Research: Earth Surface*, 123, 1–56, <https://doi.org/10.1029/2018JF004779>, 2018a.
- Beaud, F., Venditti, J., Flowers, G., and Koppes, M.: Excavation of subglacial bedrock channels by seasonal meltwater flow, *Earth Surface Processes and Landforms*, 43, 1960–1972, <https://doi.org/10.1002/esp.4367>, 2018b.
- 670 Bendixen, M., Iversen, L. L., Bjørk, A. A., Elberling, B., Westergaard-Nielsen, A., Overeem, I., Barnhart, K. R., Khan, S. A., Abermann, J., Langley, K., et al.: Delta progradation in Greenland driven by increasing glacial mass loss, *Nature*, 550, 101, <https://doi.org/10.1038/nature23873>, 2017.
- Bhatia, M. P., Kujawinski, E. B., Das, S. B., Breier, C. F., Henderson, P. B., and Charette, M. A.: Greenland meltwater as a significant and potentially bioavailable source of iron to the ocean, *Nature Geoscience*, 6, 274, 2013.
- 675 Bovy, B., Braun, J., and Demoulin, A.: A new numerical framework for simulating the control of weather and climate on the evolution of soil-mantled hillslopes, *Geomorphology*, 263, 99 – 112, <https://doi.org/https://doi.org/10.1016/j.geomorph.2016.03.016>, 2016.
- Bracken, L., Turnbull, L., Wainwright, J., and Bogaart, P.: Sediment connectivity: a framework for understanding sediment transfer at multiple scales, *Earth Surface Processes and Landforms*, 40, 177–188, <https://doi.org/10.1002/esp.3635>, <https://onlinelibrary.wiley.com/doi/abs/10.1002/esp.3635>, 2015.
- 680 Braun, J. and Willett, S.: A very efficient O (n), implicit and parallel method to solve the stream power equation governing fluvial incision and landscape evolution, *Geomorphology*, 180, 170–179, <https://doi.org/10.1016/j.geomorph.2012.10.008>, 2013.
- Brinkerhoff, D., Truffer, M., and Aschwanden, A.: Sediment transport drives tidewater glacier periodicity, *Nature Communications*, 8, 90, <https://doi.org/10.1038/s41467-017-00095-5>, 2017.
- Brinkerhoff, D. J., Meyer, C. R., Bueler, E., Truffer, M., and Bartholomaeus, T. C.: Inversion of a glacier hydrology model, *Annals of*
- 685 *Glaciology*, 57, 84–95, 2016.
- Chen, Y., Liu, X., Gulley, J. D., and Mankoff, K. D.: Subglacial Conduit Roughness: Insights From Computational Fluid Dynamics Models, *Geophysical Research Letters*, 45, 11,206–11,218, <https://doi.org/10.1029/2018GL079590>, 2018.
- Chu, W., Creyts, T. T., and Bell, R. E.: Rerouting of subglacial water flow between neighboring glaciers in West Greenland, *Journal of Geophysical Research: Earth Surface*, 121, 925–938, <https://doi.org/10.1002/2015JF003705>, 2016.
- 690 Church, M. and Ryder, J. M.: Paraglacial sedimentation: a consideration of fluvial processes conditioned by glaciation, *Geological Society of America Bulletin*, 83, 3059–3072, 1972.

- Cook, S., Swift, D., Kirkbride, M., Knight, P., and Waller, R.: The empirical basis for modelling glacial erosion rates, *Nature communications*, 11, 1–7, <https://doi.org/10.1038/s41467-020-14583-8>, 2020.
- Costa, A., Molnar, P., Stutenbecker, L., Bakker, M., Silva, T. A., Schlunegger, F., Lane, S. N., Loizeau, J. L., and Girardclos, S.: Temperature signal in suspended sediment export from an Alpine catchment, *Hydrology and Earth System Sciences*, 22, 509–528, 2018.
- 695 Covington, M. D., Gulley, J. D., Trunz, C., Mejia, J., and Gadd, W.: Moulin Volumes Regulate Subglacial Water Pressure on the Greenland Ice Sheet, *Geophysical Research Letters*, 47, e2020GL088901, <https://doi.org/https://doi.org/10.1029/2020GL088901>, <https://agupubs.onlinelibrary.wiley.com/doi/abs/10.1029/2020GL088901>, 2020.
- Cowton, T., Nienow, P., Bartholomew, I., Sole, A., and Mair, D.: Rapid erosion beneath the Greenland ice sheet, *Geology*, 40, 343–346, 2012.
- 700 Creyts, T. T., Clarke, G. K. C., and Church, M.: Evolution of subglacial overdeepenings in response to sediment redistribution and glaciohydraulic supercooling, *Journal of Geophysical Research: Earth Surface*, 118, 423–446, 2013.
- Cuffey, K. M. and Paterson, W. S. B.: *The Physics of Glaciers*, Butterworth-Heinemann, Burlington, MA, USA, Fourth edn., 2010.
- Damsgaard, A., Goren, L., and Suckale, J.: Water pressure fluctuations control variability in sediment flux and slip dynamics beneath glaciers and ice streams, *Communications Earth & Environment*, 1, 1–8, <https://doi.org/10.1038/s43247-020-00074-7>, 2020.
- 705 de Fleurian, B., Werder, M. A., Beyer, S., Brinkerhoff, D., Delaney, I., Dow, C., Downs, J., Hoffman, M., Hooke, R., Seguinot, J., and Sommers, A.: SHMIP The Subglacial Hydrology Model Intercomparison Project, *Journal of Glaciology*, 64, 897–916, <https://doi.org/10.1017/jog.2018.78>, 2018.
- Delaney, I. and Adhikari, S.: Increased subglacial sediment discharge during century scale glacier retreat: consideration of ice dynamics, glacial erosion and fluvial sediment transport, *Geophysical Research Letters*, p. e2019GL085672, <https://doi.org/10.1029/2019GL085672>, 710 2020.
- Delaney, I., Bauder, A., Huss, M., and Weidmann, Y.: Proglacial erosion rates and processes in a glacierized catchment in the Swiss Alps, *Earth Surface Processes and Landforms*, 43, 765–778, <https://doi.org/10.1002/esp.4239>, 2018a.
- Delaney, I., Bauder, A., Werder, M. A., and Farinotti, D.: Regional and annual variability in subglacial sediment transport by water for two glaciers in the Swiss Alps, *Frontiers in Earth Science*, <https://doi.org/10.3389/feart.2018.00175>, 2018b.
- 715 Delaney, I., Werder, M., and Farinotti, D.: A Numerical Model for Fluvial Transport of Subglacial Sediment, *Journal of Geophysical Research: Earth Surface*, 124, 2197–2223, <https://doi.org/10.1029/2019JF005004>, 2019.
- Egholm, D., Nielsen, S., Pedersen, V., and Lesemann, J.-E.: Glacial effects limiting mountain height, *Nature*, 460, 884–887, <https://doi.org/10.1038/nature08263>, 2009.
- Egholm, D. L., Pedersen, V. K., Knudsen, M. F., and Larsen, N. K.: Coupling the flow of ice, water, and sediment in a glacial landscape evolution model, *Geomorphology*, 141, 47–66, 2012.
- 720 Engelund, F. and Hansen, E.: A monograph on sediment transport in alluvial streams, Tech. rep., Technical University of Denmark, Copenhagen, Denmark, 1967.
- Exner, F. M.: Über die Wechselwirkung zwischen Wasser und Geschiebe in flüssen, *Abhandlungen der Akademie der Wissenschaften, Wien*, 134, 165–204, 1920a.
- 725 Exner, F. M.: Zur Physik der Dünen, *Abhandlungen der Akademie der Wissenschaften, Wien*, 129, 929–952, 1920b.
- Felix, D., Albayrak, I., Abgottspon, A., and Boes, R. M.: Suspended sediment measurements and calculation of the particle load at HPP Fieschertal, *IOP Conference Series: Earth and Environmental Science*, 49, 122007, <https://doi.org/10.1088/1755-1315/49/12/122007>, <http://stacks.iop.org/1755-1315/49/i=12/a=122007>, 2016.

- Gagliardini, O. and Werder, M. A.: Influence of an increasing surface melt over decadal timescales on land terminating outlet glaciers, *Journal of Glaciology*, 10.1017/jog.2018.59, 2018.
- 730 Geilhausen, M., Morche, D., Otto, J., and Schrott, L.: Sediment discharge from the proglacial zone of a retreating Alpine glacier, *Zeitschrift für Geomorphologie, Supplementary Issues*, 57, 29–53, <https://doi.org/10.1127/0372-8854/2012/S-00122>, 2013.
- Gimbert, F., Gilbert, A., Gagliardini, O., Vincent, C., and Moreau, L.: Do Existing Theories Explain Seasonal to Multi-Decadal Changes in Glacier Basal Sliding Speed?, *Geophysical Research Letters*, 48, e2021GL092858, <https://doi.org/10.1029/2021GL092858>, 2021.
- 735 Hairer, E., Nørsett, S. P., and Wanner, G.: Solving ordinary differential equations I: nonstiff problems, vol. 1, Springer Science & Business, <http://link.springer.com/book/10.1007/978-3-540-78862-1>, 1992.
- Hallet, B.: A theoretical model of glacial abrasion, *Journal of Glaciology*, 23, 39–50, 1979.
- Hallet, B., Hunter, L., and Bogen, J.: Rates of erosion and sediment evacuation by glaciers: A review of field data and their implications, *Global and Planetary Change*, 12, 213–235, [https://doi.org/10.1016/0921-8181\(95\)00021-6](https://doi.org/10.1016/0921-8181(95)00021-6), 1996.
- 740 Harbor, J., Hallet, B., and Raymond, C.: A numerical model of landform development by glacial erosion, *Nature*, 333, 347, 1988.
- Hawkings, J., Wadham, J., Tranter, M., Raiswell, R., Benning, L., Statham, P., Tedstone, A., Nienow, P., Lee, K., and Telling, J.: Ice sheets as a significant source of highly reactive nanoparticulate iron to the oceans, *Nature communications*, 5, 1–8, <https://doi.org/10.1038/ncomms4929>, 2014.
- Herman, F., Beaud, F., Champagnac, J., Lemieux, J. M., and Sternai, P.: Glacial hydrology and erosion patterns: a mechanism for carving glacial valleys, *Earth and Planetary Science Letters*, 310, 498–508, <https://doi.org/10.1016/j.epsl.2011.08.022>, 2011.
- 745 Herman, F., Beyssac, O., Brughelli, M., Lane, S. N., Leprince, S., Adatte, T., Lin, J. Y. Y., Avouac, J. P., and Cox, S. C.: Erosion by an alpine glacier, *Science*, 350, 193–195, <https://doi.org/10.1126/science.aab2386>, 2015.
- Herman, F., Braun, J., Deal, E., and Prasicek, G.: The Response Time of Glacial Erosion, *Journal of Geophysical Research: Earth Surface*, 123, 801–817, <https://doi.org/10.1002/2017JF004586>, <https://agupubs.onlinelibrary.wiley.com/doi/abs/10.1002/2017JF004586>, 2018.
- 750 Herman, F., De Doncker, F., Delaney, I., Prasicek, G., and Koppes, M.: The impact of glaciers on mountain erosion, *Nature Reviews Earth & Environment*, 2, 422–435, <https://doi.org/10.1038/s43017-021-00165-9>, 2021.
- Hewitt, I. and Creyts, T.: A model for the formation of eskers, *Geophysical Research Letters*, 46, 6673–6680, <https://doi.org/10.1029/2019GL082304>, 2019.
- Hewitt, I. J.: Seasonal changes in ice sheet motion due to melt water lubrication, *Earth Planetary Science Letters*, 371–372, 16 – 25, <https://doi.org/10.1016/j.epsl.2013.04.022>, 2013.
- 755 Hewitt, I. J., Schoof, C., and Werder, M. A.: Flotation and free surface flow in a model for subglacial drainage. Part 2. Channel flow, *Journal of Fluid Mechanics*, 702, 157–187, 2012.
- Hooke, R. L., Laumann, T., and Kohler, J.: Subglacial Water Pressures and the Shape of Subglacial Conduits, *Journal of Glaciology*, 36, 67–71, <https://doi.org/10.3189/S0022143000005566>, 1990.
- 760 Humphrey, N. and Raymond, C.: Hydrology, erosion and sediment production in a surging glacier: Variegated Glacier, Alaska, 1982–83, *Journal of Glaciology*, 40, 539–552, 1994.
- Hutter, K.: Theoretical glaciology, D. Reidel Publishing Co., Dordrecht, NL, <https://doi.org/10.1007/978-94-015-1167-4>, 1983.
- Iken, A. and Bindschadler, R. A.: Combined measurements of subglacial water pressure and surface velocity of Findelengletscher, Switzerland: conclusions about drainage system and sliding mechanism, *Journal of Glaciology*, 32, 101–119, 1986.
- 765 Iverson, N. R.: Laboratory simulations of glacial abrasion: comparison with theory, *Journal of Glaciology*, 36, 304–314, <https://doi.org/10.3189/002214390793701264>, 1990.

- Iverson, N. R.: A theory of glacial quarrying for landscape evolution models, *Geology*, 40, 679–682, <https://doi.org/10.1130/G33079.1>, 2012.
- Kasmalkar, I., Mantelli, E., and Suckale, J.: Spatial heterogeneity in subglacial drainage driven by till erosion, *Proceedings of the Royal Society A: Mathematical, Physical and Engineering Sciences*, 475, 20190259, <https://doi.org/10.1098/rspa.2019.0259>, 2019.
- 770 Koppes, M., Hallet, B., Rignot, E., Mouginot, J., Wellner, J. S., and Boldt, K.: Observed latitudinal variations in erosion as a function of glacier dynamics, *Nature*, 526, 100–103, 2015.
- Lane, S., Bakker, M., Costa, A., Girardclos, S., Loizeau, J.-L., Molnar, P., Silva, T., Stutenbecker, L., and Schlunegger, F.: Making stratigraphy in the Anthropocene: climate change impacts and economic conditions controlling the supply of sediment to Lake Geneva, *Scientific reports*, 9, 8904, <https://doi.org/10.1038/s41598-019-44914-9>, 2019.
- 775 Lane, S. N., Bakker, M., Gabbud, C., Micheletti, N., and Saugy, J.: Sediment export, transient landscape response and catchment-scale connectivity following rapid climate warming and alpine glacier recession, *Geomorphology*, 277, 210 – 227, <https://doi.org/10.1016/j.geomorph.2016.02.015>, 2017.
- Li, D., Lu, X., Overeem, I., Walling, D. E., Syvitski, J., Kettner, A. J., Bookhagen, B., Zhou, Y., and Zhang, T.: Exceptional increases in fluvial sediment fluxes in a warmer and wetter High Mountain Asia, *Science*, 374, 599–603, <https://doi.org/10.1126/science.abi9649>,
780 2021.
- Mancini, D. and Lane, S.: Changes in sediment connectivity following glacial debuitressing in an Alpine valley system, *Geomorphology*, 352, 106987, <https://doi.org/https://doi.org/10.1016/j.geomorph.2019.106987>, 2020.
- Mao, L., Dell’Agnese, A., Huincahe, C., Penna, D., Engel, M., Niedrist, G., and Comiti, F.: Bedload hysteresis in a glacier-fed mountain river, *Earth Surface Processes and Landforms*, 39, 964–976, <https://doi.org/10.1002/esp.3563>, 2014.
- 785 Meyer-Peter, E. and Müller, R.: Formulas for bedload transport, in: *Hydraulic Engineering Reports*, International Association for Hydro-Environment Engineering and Research, 1948.
- Micheletti, N. and Lane, S. N.: Water yield and sediment export in small, partially glaciated Alpine watersheds in a warming climate, *Water Resources Research*, 52, 4924–4943, <https://doi.org/10.1002/2016WR018774>, 2016.
- Milner, A., Khamis, K., Battin, T., Brittain, J., Barr and, N., Füreder, L., Cauvy-Fraunié, S., Gíslason, G., Jacobsen, D., Hannah, D., et al.:
790 Glacier shrinkage driving global changes in downstream systems, *Proceedings of the National Academy of Sciences*, 114, 9770–9778, <https://doi.org/10.1073/pnas.1619807114>, 2017.
- Mouginot, J., Rignot, E., Björk, A., Van Den Broeke, M., Millan, R., Morlighem, M., Noël, B., Scheuchl, B., and Wood, M.: Forty-six years of Greenland Ice Sheet mass balance from 1972 to 2018, *Proceedings of the National Academy of Sciences*, 116, 9239–9244, <https://doi.org/10.1073/pnas.1904242116>, 2019.
- 795 Nanni, U., Gimbert, F., Vincent, C., Gräff, D., Walter, F., Piard, L., and Moreau, L.: Quantification of seasonal and diurnal dynamics of subglacial channels using seismic observations on an Alpine glacier, *The Cryosphere*, 14, 1475–1496, <https://doi.org/10.5194/tc-14-1475-2020>, 2020.
- Ng, F. S. L.: Canals under sediment-based ice sheets, *Annals of Glaciology*, 30, 146–152, 2000.
- Otto, J.-C., Schrott, L., Jaboyedoff, M., and Dikau, R.: Quantifying sediment storage in a high alpine valley (Turtmanntal, Switzerland),
800 *Earth Surface Processes and Landforms*, 34, 1726–1742, <https://doi.org/https://doi.org/10.1002/esp.1856>, <https://onlinelibrary.wiley.com/doi/abs/10.1002/esp.1856>, 2009.
- Overeem, I., Hudson, B. D., Syvitski, J. P. M., Mikkelsen, A. B., Hasholt, B., van den Broeke, M. R., Noël, B. P. Y., and Morlighem, M.: Substantial export of suspended sediment to the global oceans from glacial erosion in Greenland, *Nature Geoscience*, 10, 859–863, <https://doi.org/10.1038/NGEO3046>, 2017.

- 805 Paola, C. and Voller, V. R.: A generalized Exner equation for sediment mass balance, *Journal of Geophysical Research: Earth Surface*, 110, <https://doi.org/10.1029/2004JF000274>, <https://agupubs.onlinelibrary.wiley.com/doi/abs/10.1029/2004JF000274>, 2005.
- Perolo, P., Bakker, M., Gabbud, C., Moradi, G., Rennie, C., and Lane, S. N.: Subglacial sediment production and snout marginal ice uplift during the late ablation season of a temperate valley glacier, *Earth Surface Processes and Landforms*, 0, 1–68, <https://doi.org/10.1002/esp.4562>, 2018.
- 810 Pohle, A., Werder, M. A., Gräff, D., and Farinotti, D.: Characterising englacial R-channels using artificial moulins, *Journal of Glaciology*, p. 1–12, <https://doi.org/10.1017/jog.2022.4>, 2022.
- Poinar, K., Joughin, I., Das, S., Behn, M. D., Lenaerts, J., and Broeke, M. R.: Limits to future expansion of surface-melt-enhanced ice flow into the interior of western Greenland, *Geophysical Research Letters*, 42, 1800–1807, 2015.
- Poinar, K., Dow, C., and Andrews, L.: Long-Term Support of an Active Subglacial Hydrologic System in Southeast Greenland by Firm
815 Aquifers, *Geophysical Research Letters*, 46, 4772–4781, <https://doi.org/10.1029/2019GL082786>, 2019.
- Prasicek, G., Herman, F., Robl, J., and Braun, J.: Glacial Steady State Topography Controlled by the Coupled Influence of Tectonics and Climate, *Journal of Geophysical Research: Earth Surface*, 123, 1344–1362, <https://doi.org/https://doi.org/10.1029/2017JF004559>, 2018.
- Prasicek, G., Hergarten, S., Deal, E., Herman, F., and Robl, J.: A glacial buzzsaw effect generated by efficient erosion of temperate glaciers in a steady state model, *Earth and Planetary Science Letters*, 543, 116 350, <https://doi.org/10.1016/j.epsl.2020.116350>, 2020.
- 820 Quinn, P., Beven, K., Chevallier, P., and Planchon, O.: The prediction of hillslope flow paths for distributed hydrological modelling using digital terrain models, *Hydrological processes*, 5, 59–79, 1991.
- Rackauckas, C. and Nie, Q.: DifferentialEquations.jl—A Performant and Feature-Rich Ecosystem for Solving Differential Equations in Julia, *Journal of Open Research Software*, 5, 15, <https://doi.org/10.5334/jors.151>, 2017.
- Radhakrishnan, K. and Hindmarsh, A. C.: Description and use of LSODE, the Livermore solver for ordinary differential equations, Reference
825 Publication 1327, NASA, 1993.
- Riihimäki, C. A., MacGregor, K. R., Anderson, R. ., Anderson, S. P., and Loso, M. G.: Sediment evacuation and glacial erosion rates at a small alpine glacier, *Journal of Geophysical Research: Earth Surface (2003–2012)*, 110, <https://doi.org/10.1029/2004JF000189>, 2005.
- Röthlisberger, H.: Water pressure in intra- and subglacial channels, *Journal of Glaciology*, 11, 177–203, 1972.
- Seguinot, J. and Delaney, I.: Last-glacial-cycle glacier erosion potential in the Alps, *Earth Surface Dynamics*, 9, 923–935,
830 <https://doi.org/10.5194/esurf-9-923-2021>, 2021.
- Shields, A.: Anwendung der Aehnlichkeitsmechanik und der Turbulenzforschung auf die Geschiebebewegung, PhD Thesis Technical University Berlin, 1936.
- Shreve, R. L.: Movement of water in glaciers, *Journal of Glaciology*, 11, 205–214, 1972.
- Sundal, A., Shepherd, A., Nienow, P., Hanna, E., Palmer, S., and Huybrechts, P.: Melt-induced speed-up of Greenland ice sheet offset by
835 efficient subglacial drainage, *Nature*, 469, 521, 2011.
- Swift, D. A., Nienow, P. W., and Hoey, T. B.: Basal sediment evacuation by subglacial meltwater: suspended sediment transport from Haut Glacier d’Arolla, Switzerland, *Earth Surface Processes and Landforms*, 30, 867–883, <https://doi.org/10.1002/esp.1197>, 2005.
- Tedstone, A., Nienow, P., Gourmelen, N., Dehecq, A., Goldberg, D., and Hanna, E.: Decadal slowdown of a land-terminating sector of the Greenland Ice Sheet despite warming, *Nature*, 526, 692–695, <https://doi.org/10.1038/nature15722>, 2015.
- 840 Thapa, B., Shrestha, R., Dhakal, P., and Thapa, B. S.: Problems of Nepalese hydropower projects due to suspended sediments, *Aquatic Ecosystem Health & Management*, 8, 251–257, <https://doi.org/10.1080/14634980500218241>, 2005.

- Truffer, M., Harrison, W. D., and Echelmeyer, K. A.: Glacier motion dominated by processes deep in underlying till, *Journal of Glaciology*, 46, 213–221, 2000.
- Ugelvig, S. and Egholm, D.: The influence of basal-ice debris on patterns and rates of glacial erosion, *Earth and Planetary Science Letters*, 490, 110–121, <https://doi.org/10.1016/j.epsl.2018.03.022>, 2018.
- Ugelvig, S. V., Egholm, D. L., Anderson, R. S., and Iverson, N. R.: Glacial Erosion Driven by Variations in Meltwater Drainage, *Journal of Geophysical Research: Earth Surface*, 123, <https://doi.org/10.1029/2018JF004680>, 2018.
- Wadham, J., Hawkings, J., Tarasov, L., Gregoire, L., Spencer, R., Gutjahr, M., Ridgwell, A., and Kohfeld, K.: Ice sheets matter for the global carbon cycle, *Nature communications*, 10, 1–17, <https://doi.org/10.1038/s41467-019-11394-4>, 2019.
- Walder, J. S. and Fowler, A.: Channelized subglacial drainage over a deformable bed, *Journal of Glaciology*, 40, 3–15, <https://doi.org/10.3189/S0022143000003750>, 1994.
- Weertman, J.: On the sliding of glaciers, *Journal of Glaciology*, 3, 33–38, 1957.
- Werder, M. A., Hewitt, I. J., Schoof, C. G., and Flowers, G. E.: Modeling channelized and distributed subglacial drainage in two dimensions, *Journal of Geophysical Research: Earth Surface*, 118, 2140–2158, <https://doi.org/10.1002/jgrf.20146>, 2013.
- Willis, I. C., Richards, K. S., and Sharp, M. J.: Links between proglacial stream suspended sediment dynamics, glacier hydrology and glacier motion at Midtdalsbreen, Norway, *Hydrological Processes*, 10, 629–648, 1996.
- Wohl, E., Brierley, G., Cadol, D., Coulthard, T., Covino, T., Fryirs, K., Grant, G., Hilton, R., Lane, S., Magilligan, F., Meitzen, K., Passalacqua, P., Poeppl, R., Rathburn, S., and Sklar, L.: Connectivity as an emergent property of geomorphic systems, *Earth Surface Processes and Landforms*, 44, 4–26, <https://doi.org/10.1002/esp.4434>, 2019.
- Zechmann, J., Truffer, M., Motyka, R., Amundson, J., and Larsen, C.: Sediment redistribution beneath the terminus of an advancing glacier, Taku Glacier (T'aakú Kwáan Sít'i), Alaska, *Journal of Glaciology*, p. 1–15, <https://doi.org/10.1017/jog.2020.101>, 2020.

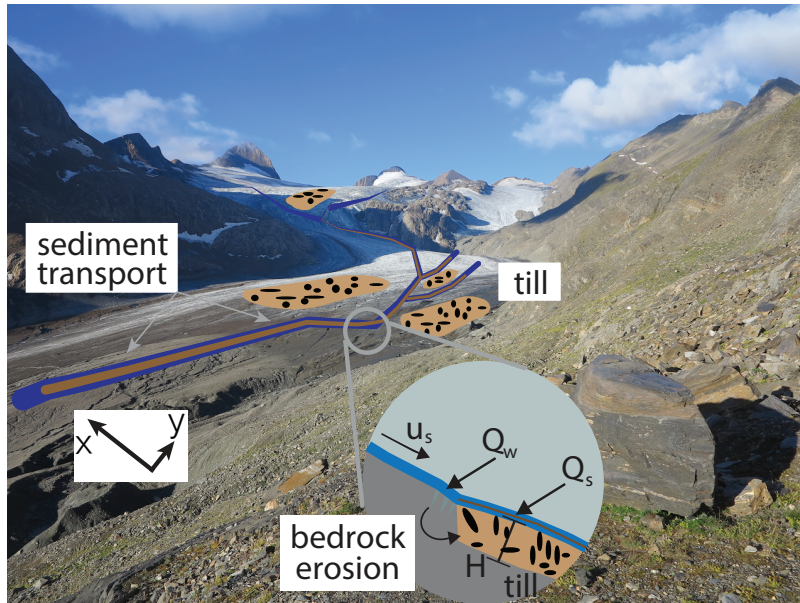


Figure 1. Cartoon of erosional and sediment transport processes considered in model below image of Griesgletscher in 2016. Bedrock erosion scales with sliding speed (u_s) and adds material to the till layer with thickness H , while water (Q_w) transports sediment (Q_s) fluvially, if sediment persists in that location of the glacier bed and fluvial transport conditions are sufficient.

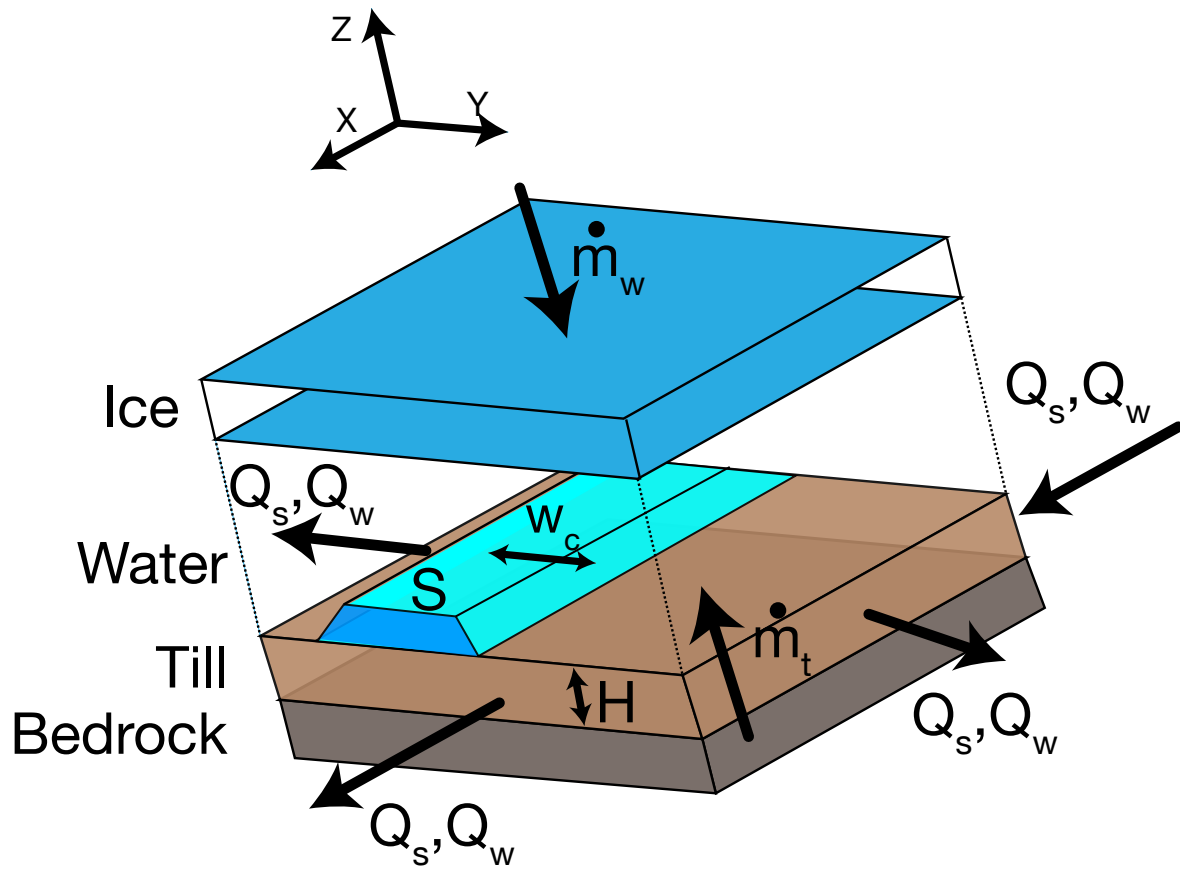


Figure 2. Illustration of terms in Equation 7, detailing the layers of bedrock, till, water and ice. Characteristics of the subglacial channel are also noted, but shown in one dimension for clarity.

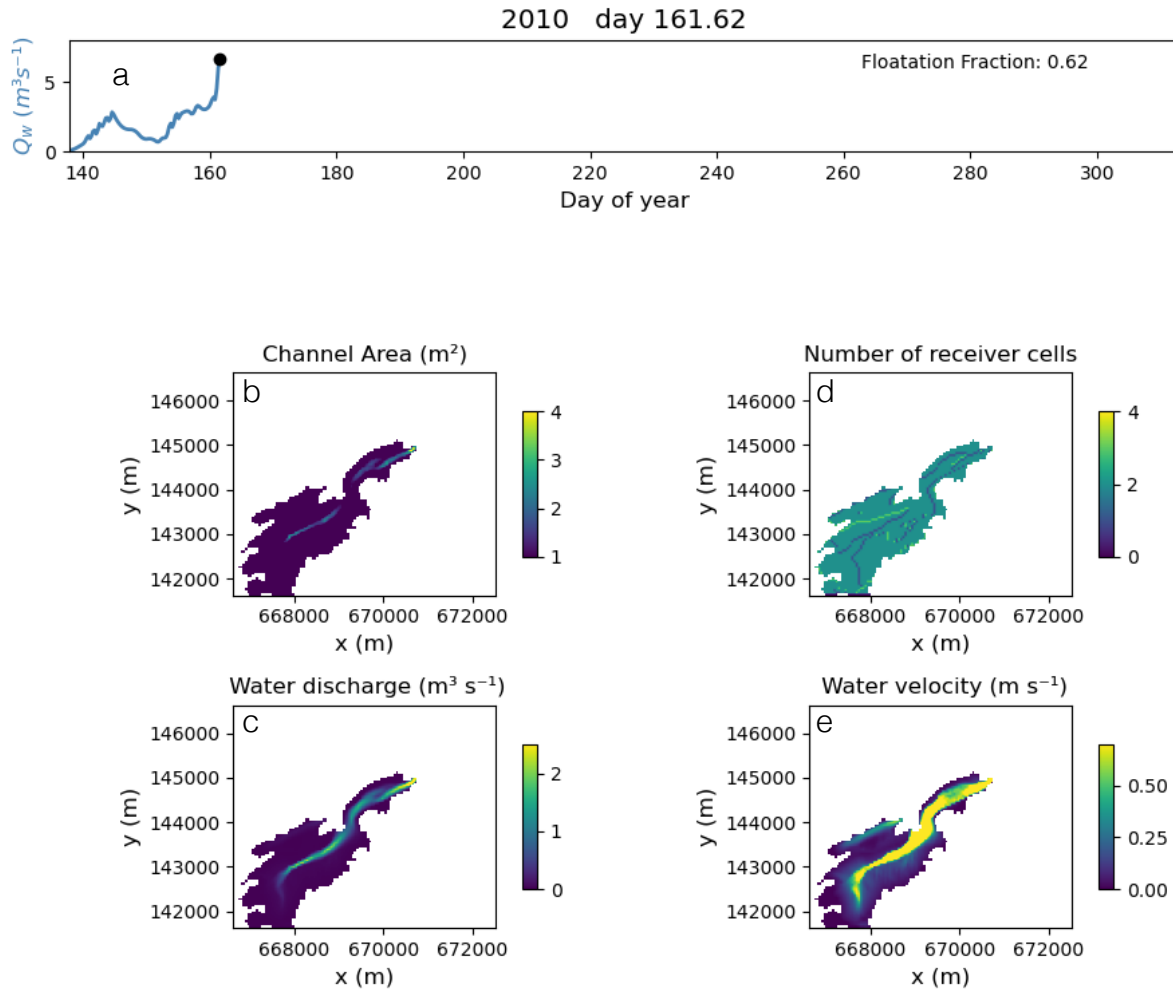
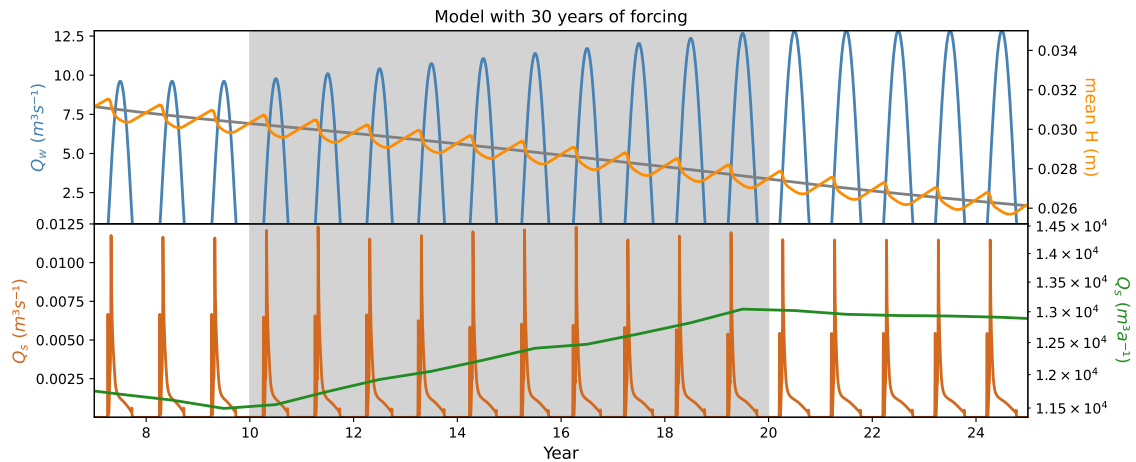


Figure 3. Example of model parameters and variables for the snap-shot of the Griesgletscher test-case Section 3.2. Water discharge from the catchment and glacier flotation fraction (a). Channel cross-sectional area S (b) with distributed water discharge (c), the number of receivers cells, r_t for a given cell (d), and the water velocity (e). Conditions b-d evolve with different hydrological conditions (e.g. a) over the glacier run. High water velocities persist at this time step due to rapid increase in water discharge (a).

Mass conservation test (a, b), sediment export volumes (c, d) and wall-time on a single processor (e,f) for a variety of solving tolerances and cell sizes. Note that $reltol$ and $abstol$ are equal (Table 3). A diurnal forcing with no seasonal variation was applied to the synthetic alpine glacier case (Section 3.1).



Model

output from an ice sheet topography over a 20-year run with diurnal variations in melt to moulin inputs. Diurnal values averaged for clarity.

Top panel a) represents water discharge (Q_w) and mean till height (H). Lower panel b) shows sediment discharge capacity (Q_{sc}) and sediment discharge (Q_s).

Spatial view of subglacial sediment transport (a), water discharge (c), till layer height prior to increased melt (b) and after increased melt (d). Blue ovals denote places of increased sediment uptake and subsequent decreased uptake due to sediment transport capacity.

Figure 4. Model output from alpine topography and forcing over a 30 year run with diurnal and seasonal variations in melt input. Grey box represents time period of increasing glacier melt. a) Seasonally varying water discharge (Q_w) increases from year 12 to 20, while till height (H) decreases. b) Sediment discharge increases over this time period, with highest sediment discharge occurring in years 14–17 when increasing glacier melt can access new sediment sources high on the glacier. Following the increase in temperature, melt persists year around, so sediment accumulated during the winter months is no longer available, and thus the glacier does not experience periods of high sediment discharge, although annual sums might be higher.

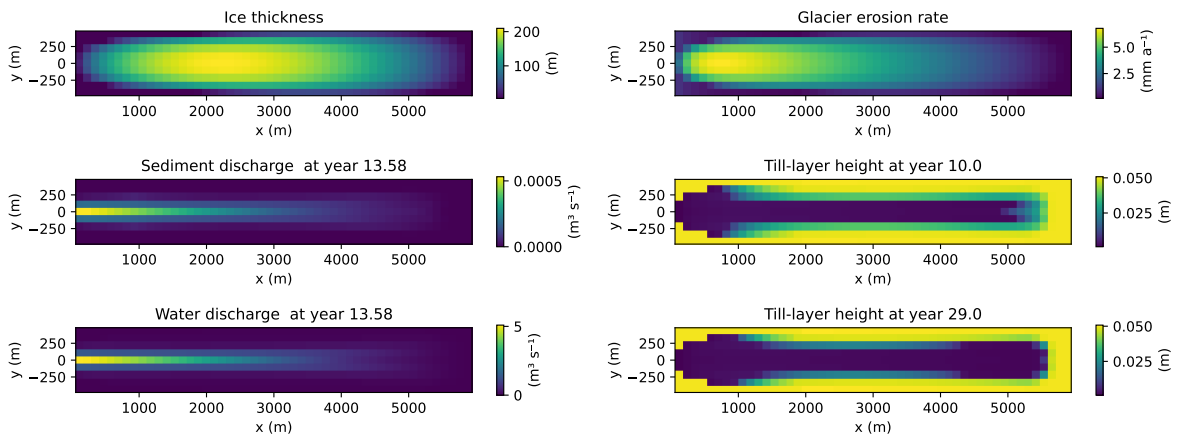


Figure 5. Spatial view of subglacial sediment transport (a), water discharge (c), till layer height prior to increased melt (b) and after increased melt (d). Spatial discontinuities in the distribution of water and sediment discharge in plots a) and c) result from the depletion of subglacial till beneath the glacier. Following the increase in melt, sediment transport increased so that it exceeded bedrock erosion. We have included an animation of this figure in the video supplement.

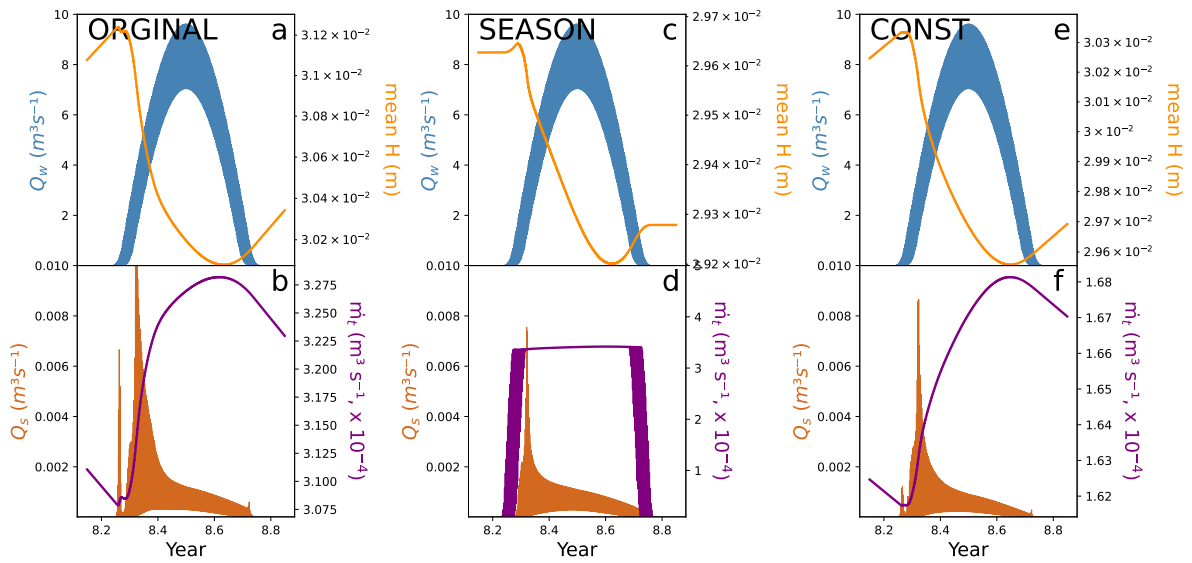


Figure 6. Annual response to different erosion patterns across the glacier, although diminishing bedrock erosion with respect to till-height till height is still in place given Equation 12. (a,b) Conventional model setup, where sediment is produced year around. This results in the peak amounts of sediment discharge occur in scenario 1 (a,b) where large amounts of sediment accumulated at the glacier terminus during the winter months. (c,d) Equivalent setup to previous, except sediment is only produced in summer months, when water is present at the glacier bed. Thus, till-height till height remains constant over the winter months. (e,f) Steady erosion of 1 mm a^{-1} across the entire glacier, with no spatial or temporal variability in sediment production. Yet, the different bedrock erosion scenarios each demonstrate increased sediment discharge at the onset of melt and subsequent exhaustion over the course of the season.

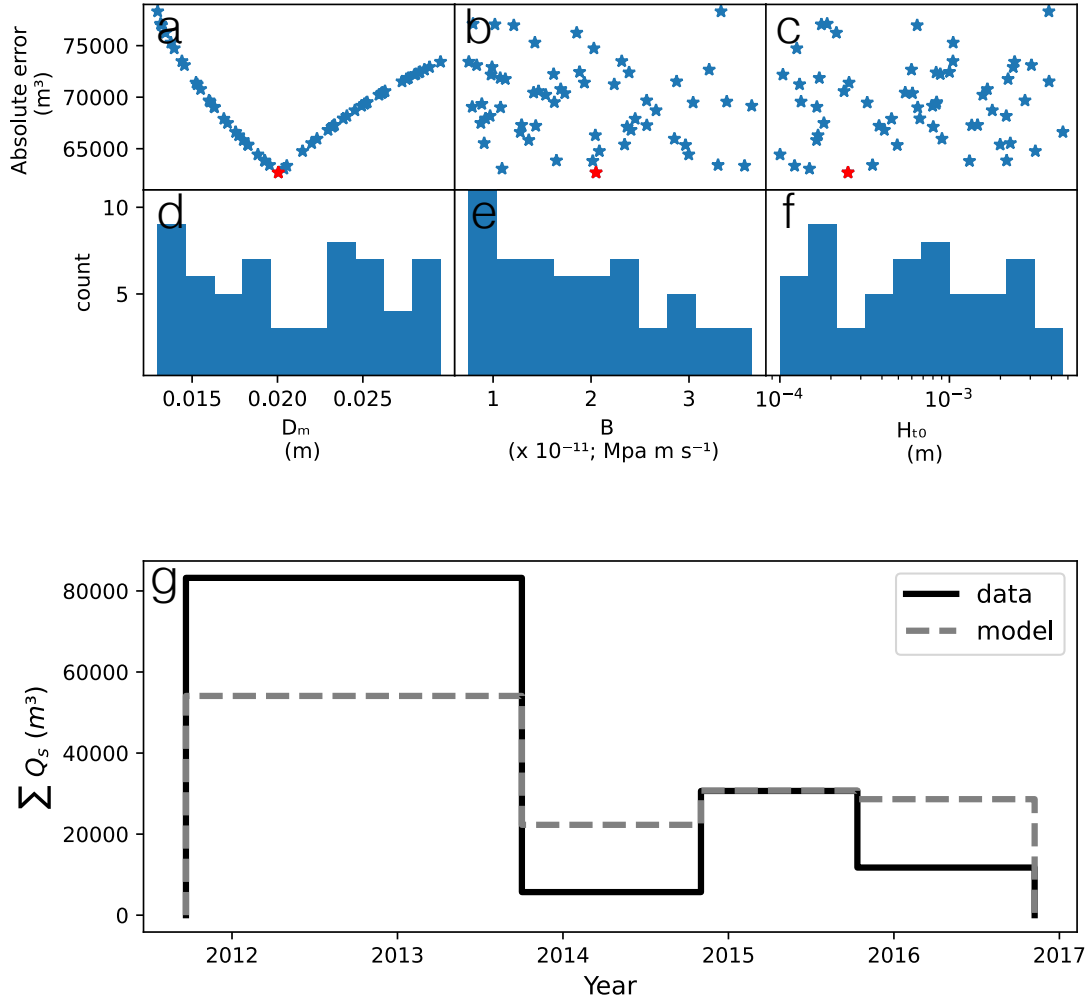


Figure 7. Results of the parameter search (column 1), the frequency of parameter values that produced a rank correlation of 1 (column 2) and the best fit model run amongst the parameter combinations (column 3). The model *hikely* fails to adequately capture the 2012–2013 period probably due to processes not considered in the framework.

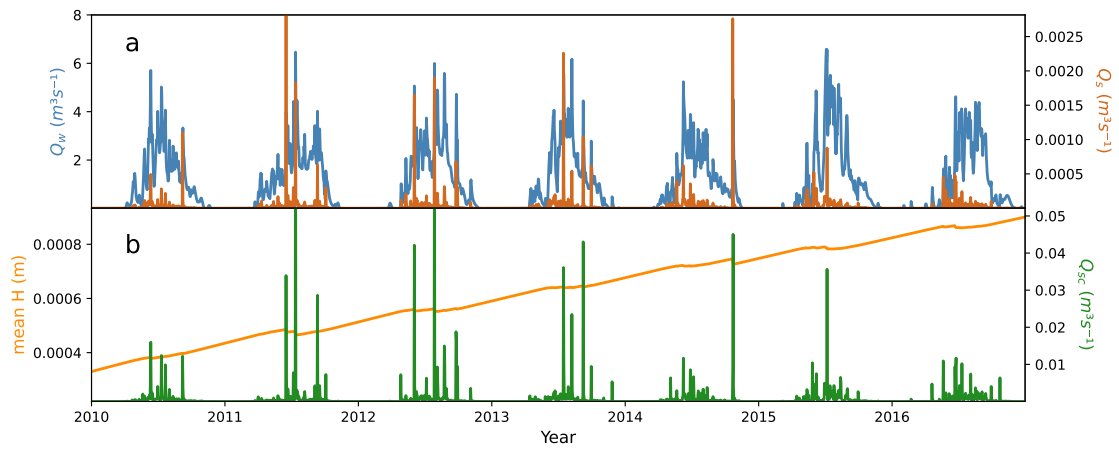


Figure 8. Sediment-Water discharge, an input modeled for Griesgletscher in (Delaney et al., 2018b), and water-sediment discharge, output of the model, from Griesgletscher (a) and. Below is modeled outputs of sediment transport capacity and average till height (b). Note that sediment discharge capacity is roughly one order of magnitude larger than sediment transport discharge. Additionally, the reduction in till height H through this model run shows that sediment is transported from the glacier bed at a greater rate than it is produced.

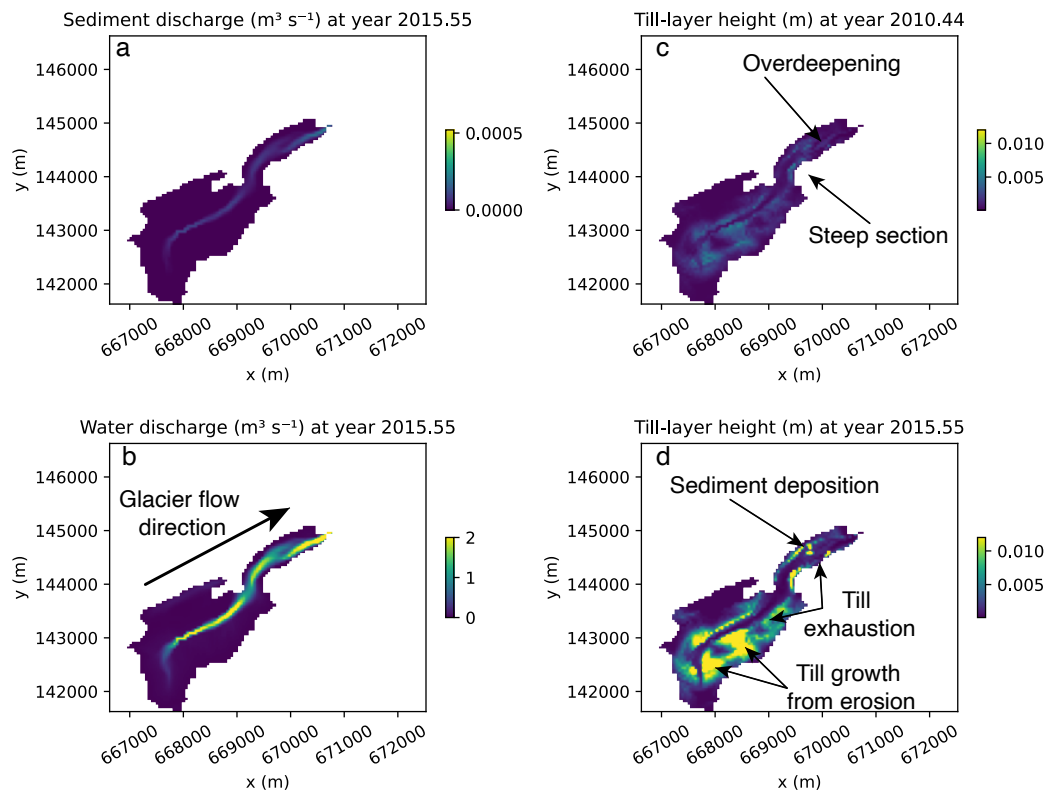


Figure 9. Spatial view of characteristics from the select Griesgletscher model run. Figure 1 shows images of this glacier. Subglacial sediment transport (a) and water discharge (c) are highly variable across the bed. Till layer height change substantially from the beginning of the model run (c) to after the model run (d). We point out the over-deepening near the glacier terminus as well as as a steep section connected the upper and lower glacier. Over this time till exhaustion in regions of high water flow are visible, while regions of sediment deposition and till growth from glacier erosion can be identified. We have included an animation of this figure in the video supplement.

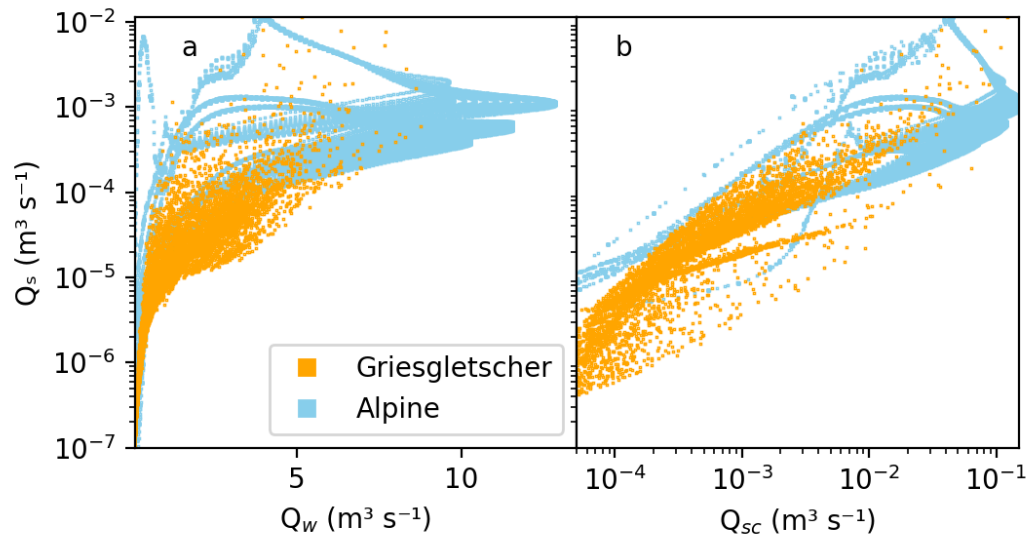


Figure 10. Model outputs of sediment discharge from the glacier compared to water discharge (a) and sediment transport capacity (b).

Table 1. Model variables

Name	Symbol	Units
Horizontal (x,y) , vertical and time coordinates	x, y, z, t	m, m, m, s
Surface and bed elevation	z_s, z_b	m, m, m
Glacier surface slope	α	-
Channel hydraulic diameter	D_h	m
Width of channel floor	w_c	m
Channel cross-sectional area	S	m ²
Water discharge (instantaneous)	Q_w	m ³ s ⁻¹
Water source term	\dot{m}_w	m s ⁻¹
Representative water discharge	Q_w^*	m ³ s ⁻¹
Hydraulic potential	ϕ	Pa
Gradient of ϕ	Ψ	Pa m ⁻¹
Flotation fraction f_f -Representative gradient of ϕ	Ψ^*	Pa m ⁻¹
<u>Flotation fraction</u>	f_t	-
Water velocity	v	m s ⁻¹
Water shear-stress	τ	Pa
Till source term	\dot{m}_t	m s ⁻¹
Sediment discharge	Q_s	m ³ s ⁻¹
Sediment discharge capacity	Q_{sc}	m ³ s ⁻¹
Glacier sliding velocity	u_b	m s ⁻¹
Erosion rate	\dot{e}	m s ⁻¹
Till layer height	H	m
Mass-balance rate at terminus	\dot{b}^0	m s ⁻¹

Table 2. Physical model parameters and constants

Name	Symbol	Value	Units
Darcy-Weisbach friction factor	f_r	<u>Alpine: 15; Gries: 5</u>	-
Hooke angle of channel	β	22.5	°
Source quantile -percentile	$s_q s_p$	<u>Alpine: 0.75(;</u> Gries: .2)	-
Source average time		2.5 (Alpine: 1.5; Gries: 0.5)	d
Sediment-uptake e -folding length	l	100 (Ice sheet: 500)	m
Sediment grain mean diameter	D_{m50}	5×10^{-4} (Gries: 0.014)	m
Till height limit	H_{lim}	0.10	m
Till height erosion limit	H_g	0.05	m
Gravitational constant	g	9.81	m s^{-2}
Density of water	ρ_w	1000	kg m^{-3}
Density of ice	ρ_i	900	kg m^{-3}
Density of bedrock	ρ_b	2650	kg m^{-3}
Bulk density of sediment	ρ_s	1500	kg m^{-3}
Erosional exponent	l_{er}	2.02 ^a	-
Erosional constant	k_g	2.7 ^{-7 a}	$\text{m}^{1-l_{er}} \text{s}^{l_{er}-1}$
Seconds per year	s_{year}	3.1536 ⁷	s
Seconds per day	s_{day}	86,400	s
Glen's n	n	3	-
Ice flow rate factor	A	2.4×10^{-24}	s Pa^{-3}
Mass-balance gradient	γ	0.00625	a^{-1}
Basal melt rate	\dot{m}_b	7.3×10^{-11}	m s^{-1}
Glacier sliding fraction -Sliding rate factor	$f_{st} B$	<u>3.2×10^{-12}</u>	<u>MPa m s^{-1}</u>
<u>Sliding exponent</u>	<u>m</u>	1(Gries: 4.09)	-

Table 3. Numerical model parameters

Name	Symbol	Value	Units
Solver tolerance (relative)	reltol	10×10^{-8}	-
Solver tolerance (absolute)	abstol	10×10^{-8}	m
Maximum timestep	dtmax	21600 (6)	s (hr)
Minimum timestep	dtmin	1	s
Edge length (x)	ds		m
Edge length (y)	dh		m
Cell area	δ		m ²
Sediment connectivity factor	$\Delta\sigma$	10^{-3}	m
Minimum hydraulic diameter <u>cross-section</u>	D_{hmin} <u>S_{min}</u>	0.3 <u>0.5</u>	m
Number of cells	n_n	-	-
Stack	s_t	\vec{n}_n	-
Receivers	r_s	$4 \times n_n$	-
Number of receivers per cell	n_r	\vec{n}_n	-
Donors	d_n	$4 \times n_n$	-
Number of donors per cell	n_d	\vec{n}_n	-
Weight of each receiver	w_r	$4 \times n_n$	-